



Институт ядерной физики
имени Г. И. Будкера СО РАН



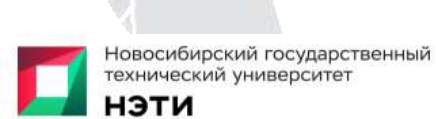
ОИЯИ



НАЦИОНАЛЬНЫЙ
ИССЛЕДОВАТЕЛЬСКИЙ ЦЕНТР
«КУРЧАТОВСКИЙ ИНСТИТУТ»



НИЯУ
МИФИ



Новосибирский государственный
технический университет

НЭТИ



UNIVERSIDAD
PABLO DE
OLAVIDE
SEVILLA

N* Новосибирский
государственный
университет
*НАСТОЯЩАЯ НАУКА



VNiVERSiDAD
D SALAMANCA

Development of experimental research program for multi-quark systems at high p_T on Nuclotron

High P_t @ Nuclotron

A. Stavinsky¹ for Niptan group (stavinsk@jinr.ru)

Г. Шарков², П. Алексеев^{1,6}, С. Алиева¹, Е. Антохин³, С. Афанасьев¹,
М. Барабанов¹, А. Барняков^{3,4,5}, Т. Бедарева³, В. Блеко¹, О. Валов³, А. Галоян¹,
Д. Дряблов¹, Н. Жигарева⁶, К. Жолдасбеков¹, Р. Ледницки¹, А. Мартемьянов⁶,
Р. G. Ortega⁸, В. Плотников¹, Н. Пухаева¹, О. Рогачевский¹, Т. Рыбаков², Д. Сакулин¹, J.
Segovia⁷, В. Стеханов⁶, Г. Таэр⁶, В. Ужинский¹, Э. Фахрутдинов², **С. С. Шиманский¹**,
Р. Шиндин¹, Т. Эник¹

¹ ОИЯИ, ² НИЯУ МИФИ, ³ ИЯФ СО РАН, ⁴ НГУ, ⁵ НГТУ, ⁶ НИЦ КИ, ⁷ Universidad Pablo de Olavide, Sevilla, Spain, ⁸ Universidad de Salamanca, Spain

Status EOI(expression of interest)

Russia:

Omsk (Omsk State Transport University: Sosnovskiy Yu.M., Kurmanov R.S.)

Omsk (Dostoevsky Omsk State University: Potudanskaya M.G., Strunin V.I.)

Mexico:

Morelia (Michoacan University of San Nicolás de Hidalgo: Diaz A.-R.)

Japan:

Osaka (Research Center for Nuclear Physics, Osaka University: Hosaka A.)

China:

Beijing (University of Chinese Academy of Sciences: Olsen S.)

Beijing (Center High Energy Physics, Tsinghua University: Bingsong Z.)

Создание ускорительной базы ЛФВЭ ОИЯИ:

- 1993: под руководством акад. А.М. Балдина создан Нуклотрон – **первый** в мире СП синхротрон тяжелых ионов (4,5 АГэВ) на основе передовой технологии «Дубненских» СП магнитов, востребованных как для ускорительных центров, так и для прикладных целей;

- 2009: решением КПП ОИЯИ началась реализация проекта **NICA – Nucloton based Ion Collider Facility**:

- 2016: подписано Соглашение между ОИЯИ и Правительством РФ о создании и эксплуатации Комплекса **NICA**

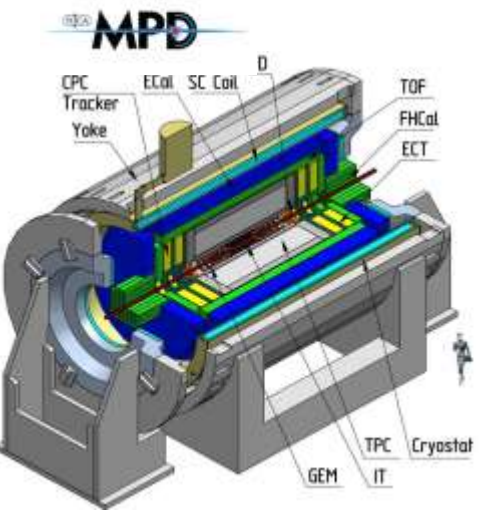


- 2018: Мегасайенс проект **Комплекс NICA** вошел в состав Национального проекта РФ НАУКА

Разработана научная программа **NICA**, нацеленная на исследование: **КХД** диаграммы в мало изученной области **большой** барионной плотности, где **КХД** на решетке не эффективна; **спиновой структуры** нуклонов; а также широкого спектра прикладных работ.

2018: Начато формирование международных научных коллабораций

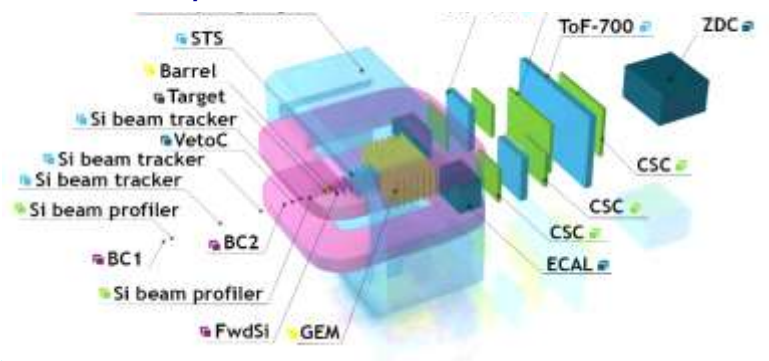
Multi Purpose Detector (MPD) Collaboration:



12 стран + ОИЯИ,
39 центров;
> 500 участников;
завершается создание детектора,
подготовка к набору данных

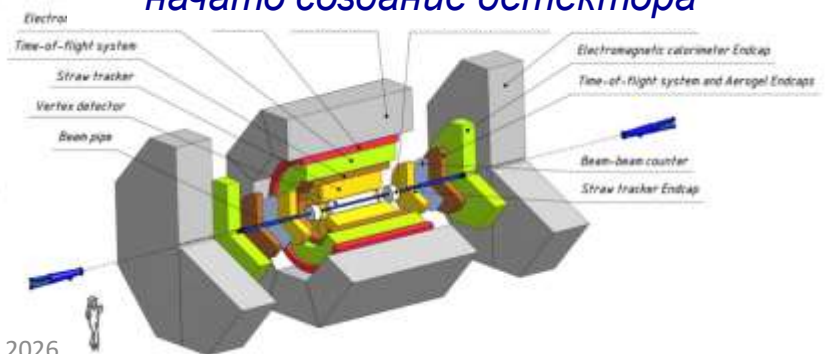
Baryonic Matter at Nuclotron (BM@N) :

5 стран + ОИЯИ, 13 центров, >220 участников;
начаты эксперименты



Spin Physics Detector (SPD) Collaboration:

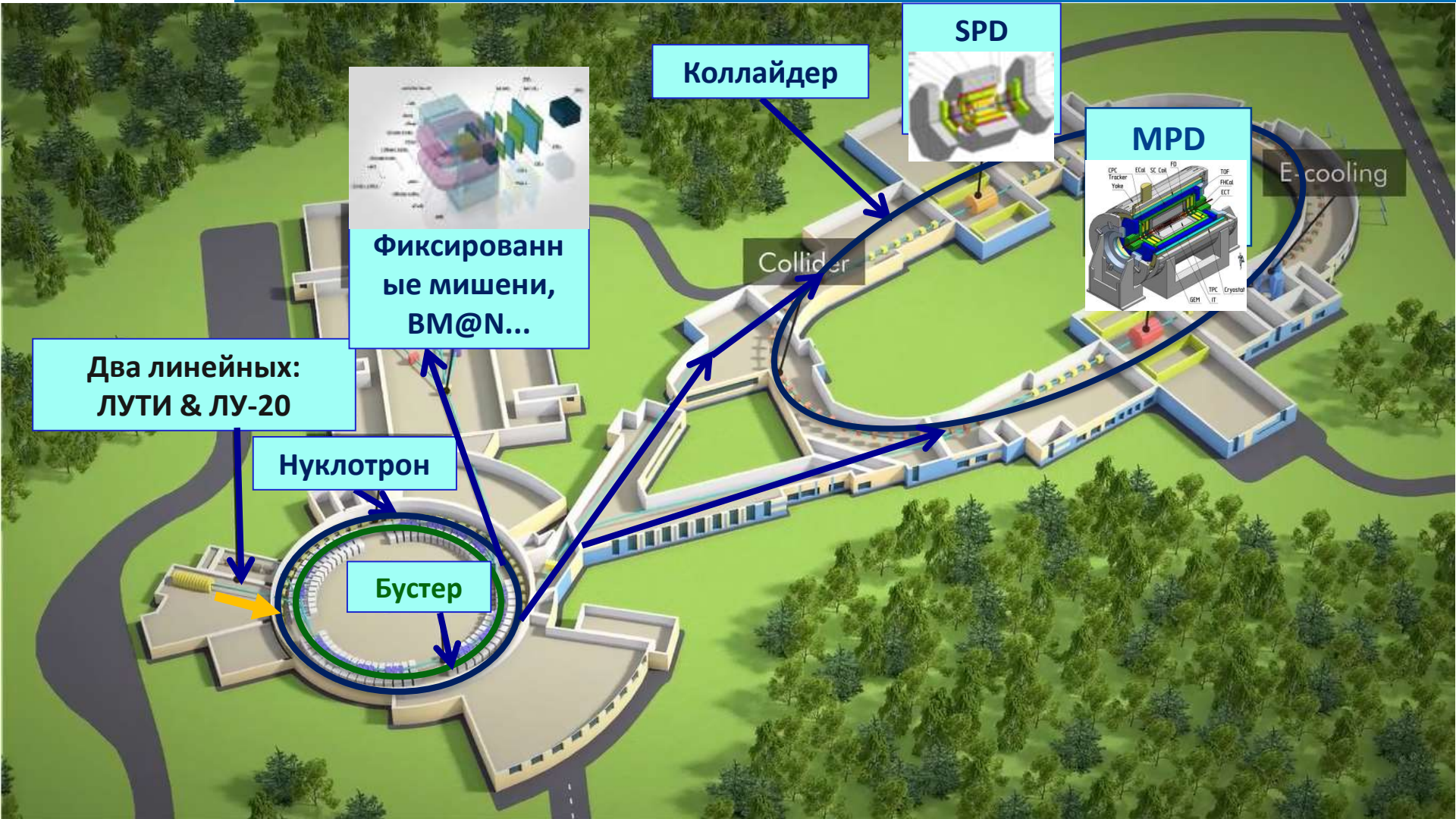
12 стран+ОИЯИ, 35 центров,
> 300 участников;
начато создание детектора



Коллаборация ARIADNA



для прикладных и инновационных работ:
6 стран, 27 центров, > 185 участников;
начаты исследования



Motivation: Nuclotron is a good choice for rare processes with $p_T > 1$ GeV/c investigations

Maximal E_p 12 GeV

Maximal $E_A(q/A=0.5)$ 6 GeV

Intensity (p) per spill 2 sec **up to 10^{10}**

Time to fill the NICA rings **0.5 h**

Collisions on NICA **3 h**

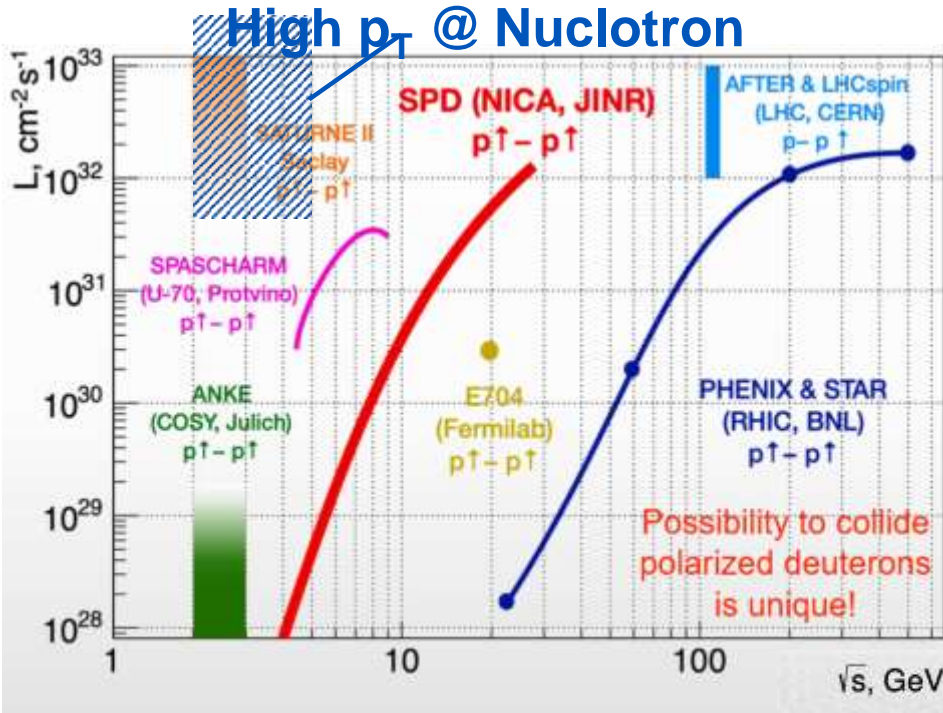
Polarized beams $p\uparrow, d\uparrow, {}^3\text{He}\uparrow$

Between NICA cycles Nuclotron will give beams to fixed target experiments

+ Polarized and cryogenic targets

MPD + BM@N

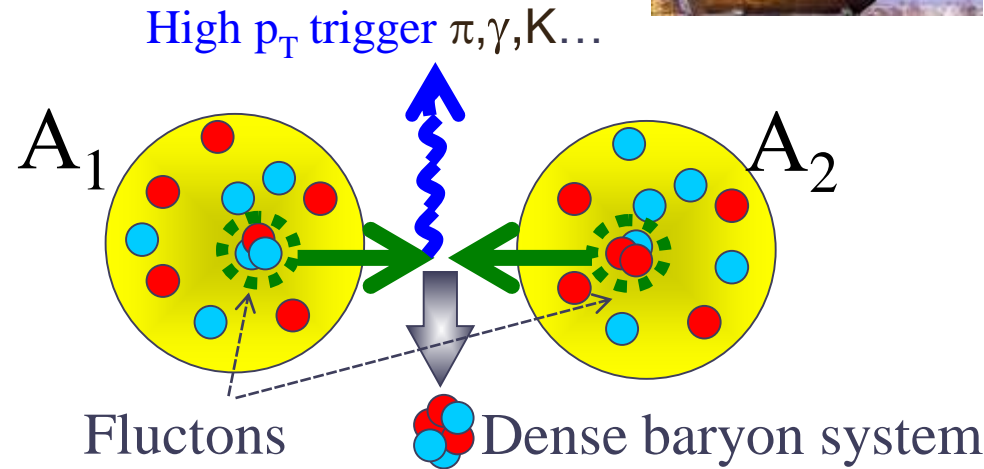
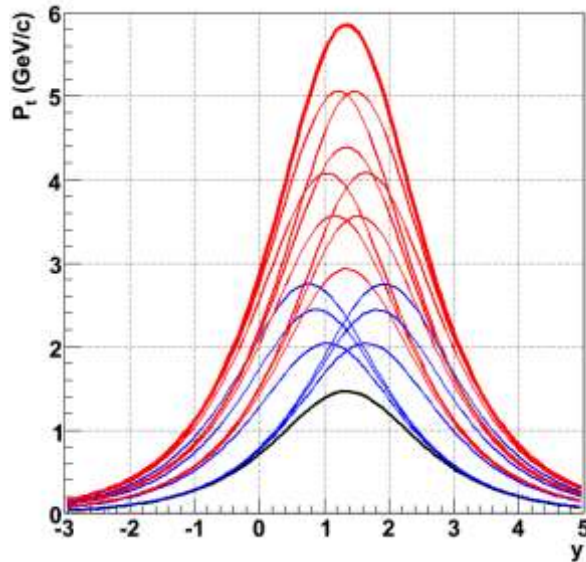
SPD + ? (High p_T @ Nuclotron)



Why high p_t ?



Scheme of A_1+A_2 process, A_i : d(up to $2N+2N$), He, C, ...



Trigger particle kinematical limits for different subprocesses: $1N+1N$ (black line)

$1N+Flucton(2N,3N,4N)$ & $Flucton+1N$ (blue lines)

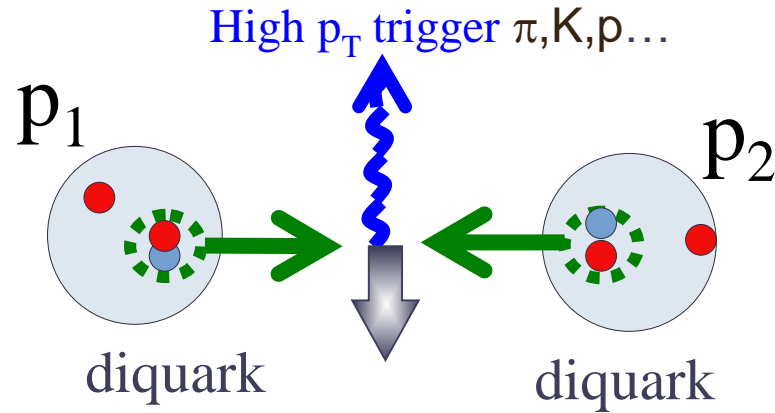
$Flucton+Flucton$ (red lines)

(6A GeV fixed target)

$$p_t(\max)(iN+iN) \sim p_t(\max)(N+N)$$

Why high p_t ?

Scheme of p_1+p_2 process



The same logic for PP:

$p_t(\text{max})(\text{diquark}+\text{diquark}) > p_t(\text{max})(\text{quark}+\text{quark})$



Diquarks

Anomaly at $p_T=2$ GeV/C seen in p/π also

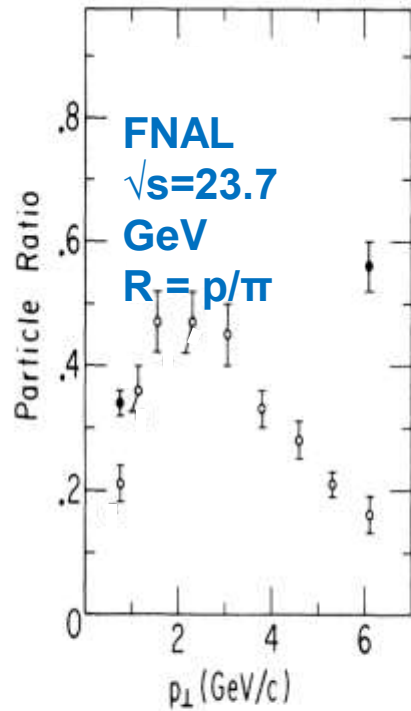
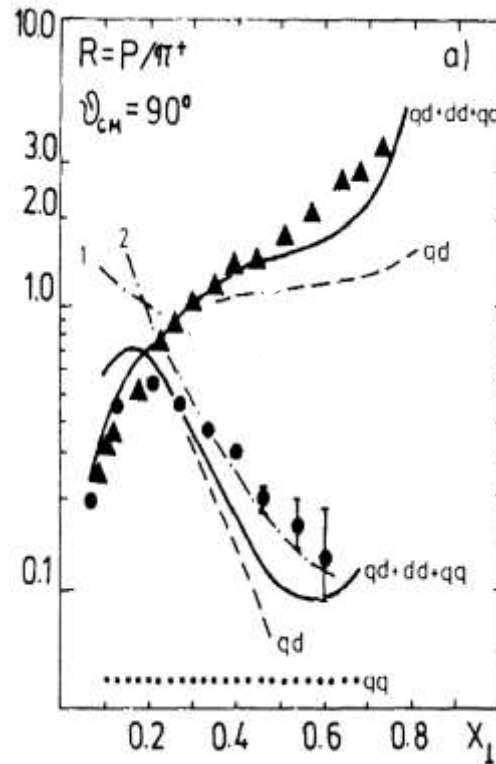


FIG. 20. Comparison of the cross-section ratio p/π^+ measured on tungsten at $\sqrt{s}=23.7$ GeV (closed circles), with that obtained by extrapolation to $A=1$ (open circles). Ratios obtained from the British-Scandinavian collaboration (Ref. 23) at $\sqrt{s}=23.4$ GeV are also plotted (closed squares).

FNAL Cronin et. Al. Phys Rev d11 (1975) 3105

Description of this anomaly using diquarks



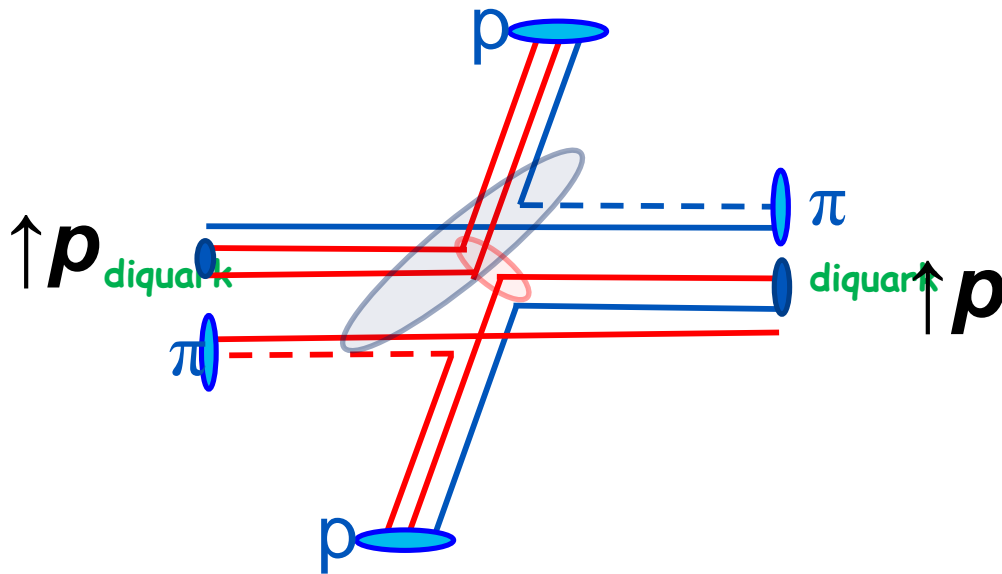
$$x_{\perp} = 2p_{\perp}/\sqrt{s}.$$

V.T. Kim
"Diquarks and dynamics of large- p_T baryon production"

V.T. Kim Mod. Phys Lett A 3 9 (1988) 909

Measurements of A_{nn} in pp , πp and $\pi\pi$ scatterings would give indication on diquark spin

Exclusive reactions at high p_T



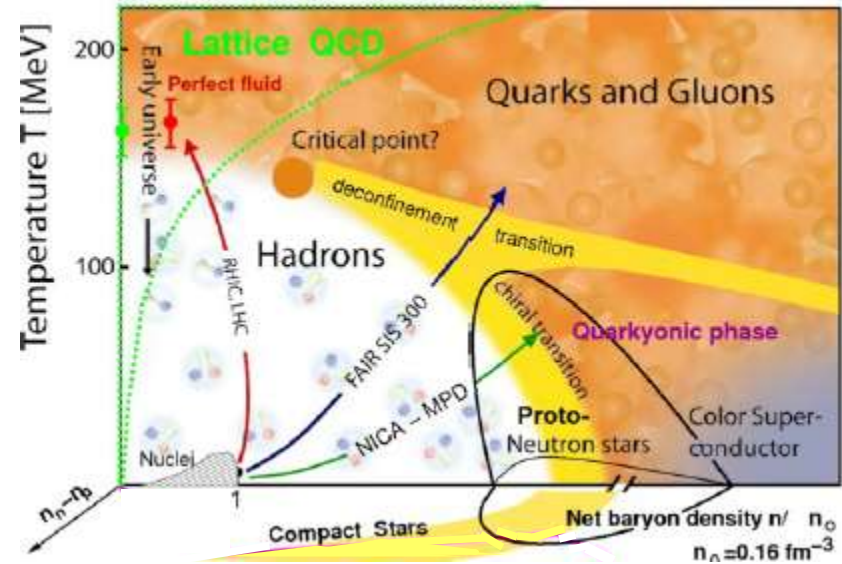
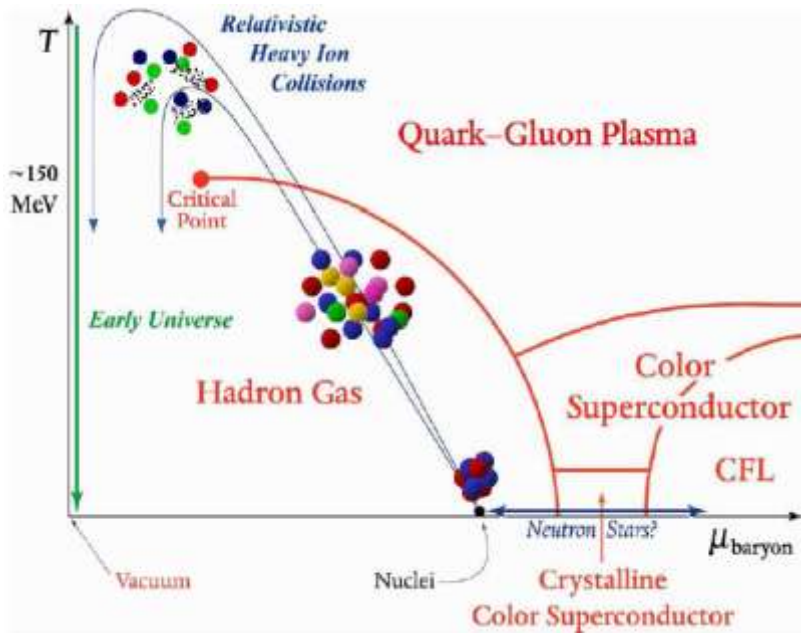
$$A_{n(pp)} \rightarrow 0 \text{ Diquark } (S=0)$$

$$A_{nn(pp)} \neq 0 \rightarrow dd \text{ (} S_d=1 \text{)}$$

$$A_{nn(\pi p)} \neq 0 \rightarrow qd \text{ (} S_d=1 \text{)}$$

$$A_{nn(\pi\pi)} \neq 0 \rightarrow qq$$

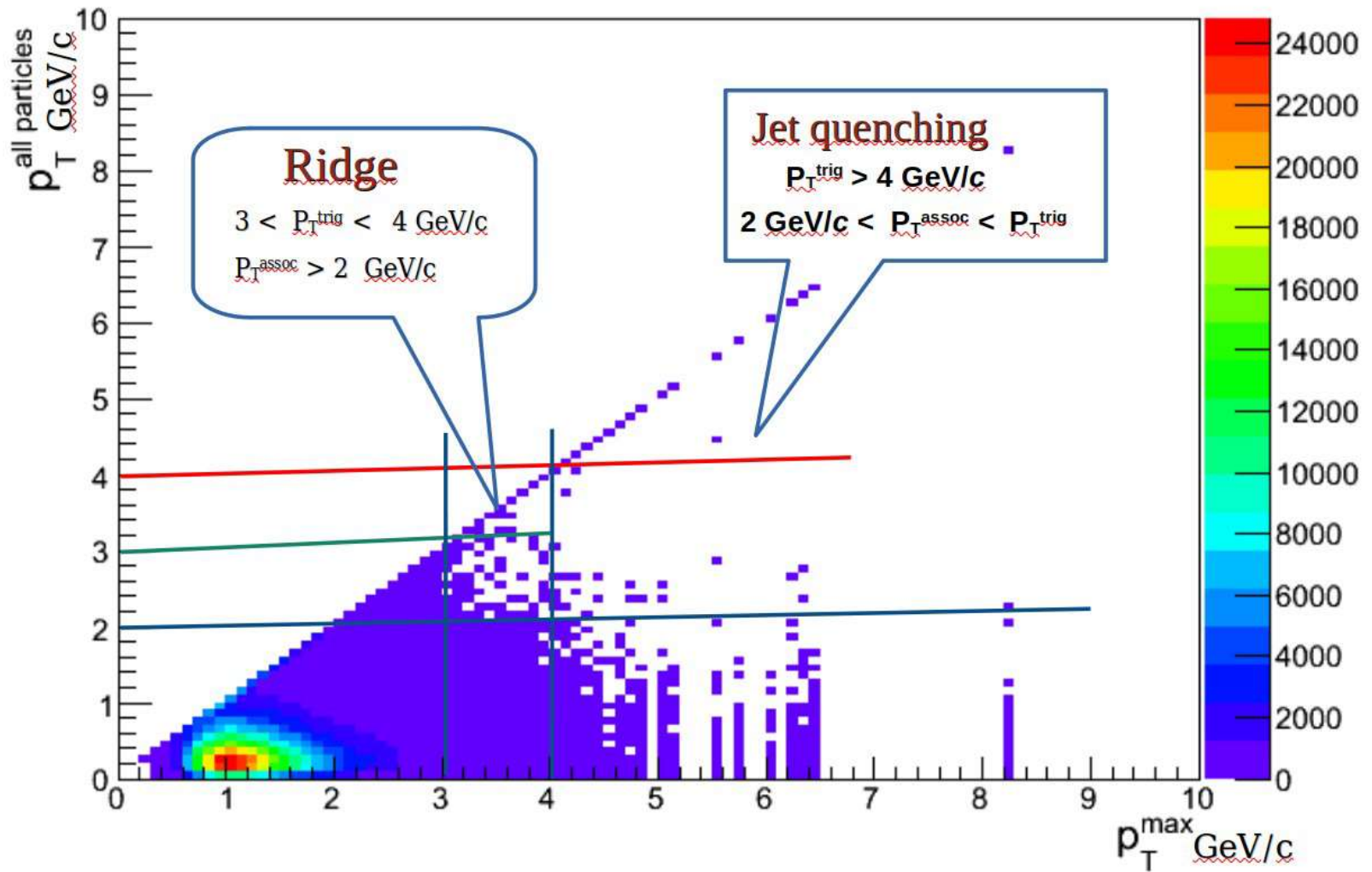
Phase diagram of nuclear matter



* $\rho/\rho_0 \gg 1$, $T/T_0 \ll 1$ (**D**ense **C**old **M**atter): rich structure of the QCD phase diagram - new phenomena are expected!

** Diagram study not finished - additional new phenomena can be found

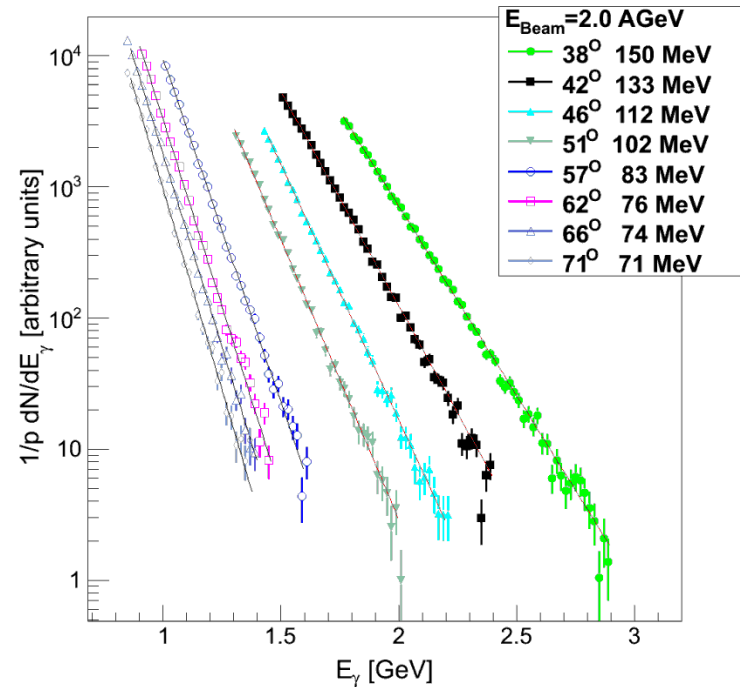
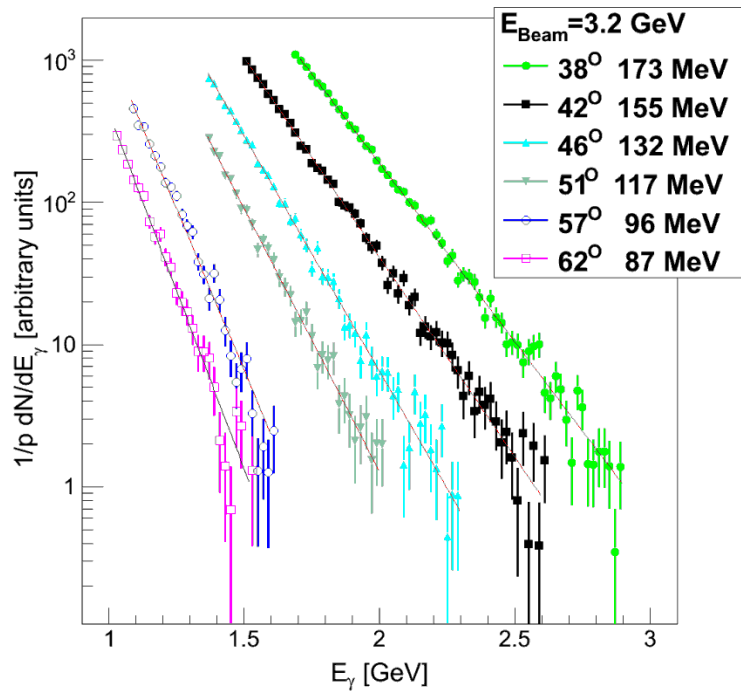
See, for example L. McLerran, "Happy Island", arXiv:1105.4103 [hep-ph] and ref. therein.



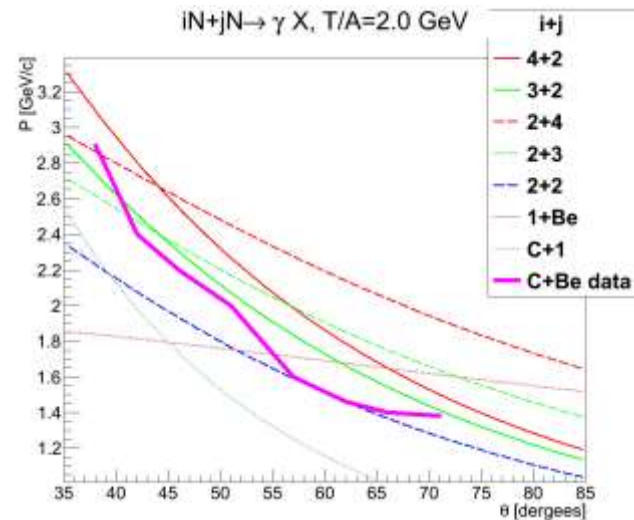
STAR AuAu $\sqrt{s_{\text{NN}}}=200$ GeV;
 O.Rogachevsky, VBLPHE-seminar,08.04.2026

Why Nuclotron?

FLINT DATA: Photon spectra $CBe \rightarrow \gamma X$



FLINT have got data for **flucton-flucton** interaction up to 6 nucleons kinematical region, which cannot be explained neither p+Be nor C+p interactions
 Six nucleons system: n!n!p!p!+??
 Does we already see phase transition?



Femtoscscopy

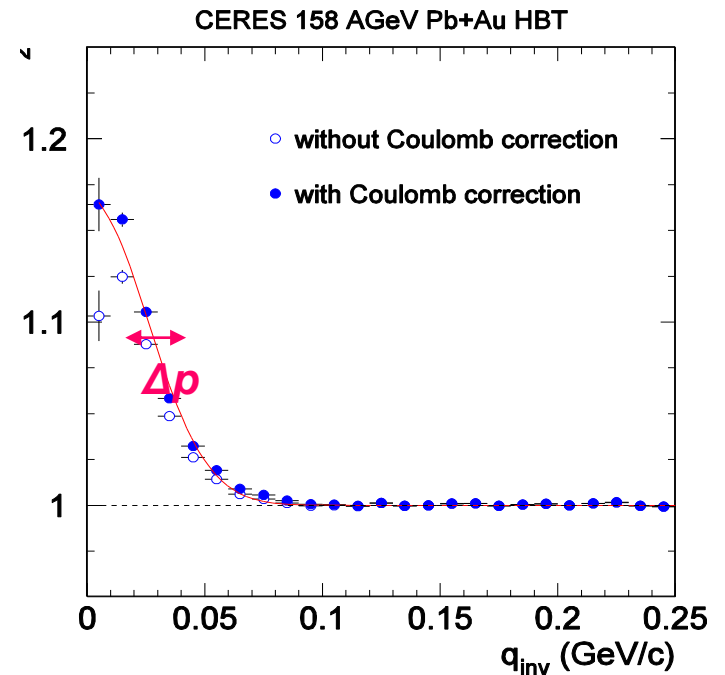
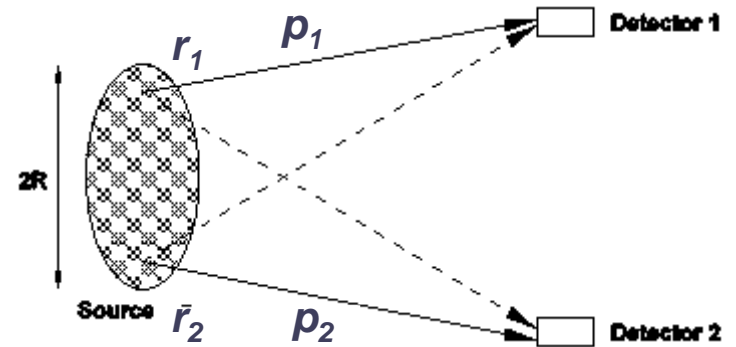
Bose-Einstein statistics of identical bosons leads to short-range correlations in momentum space

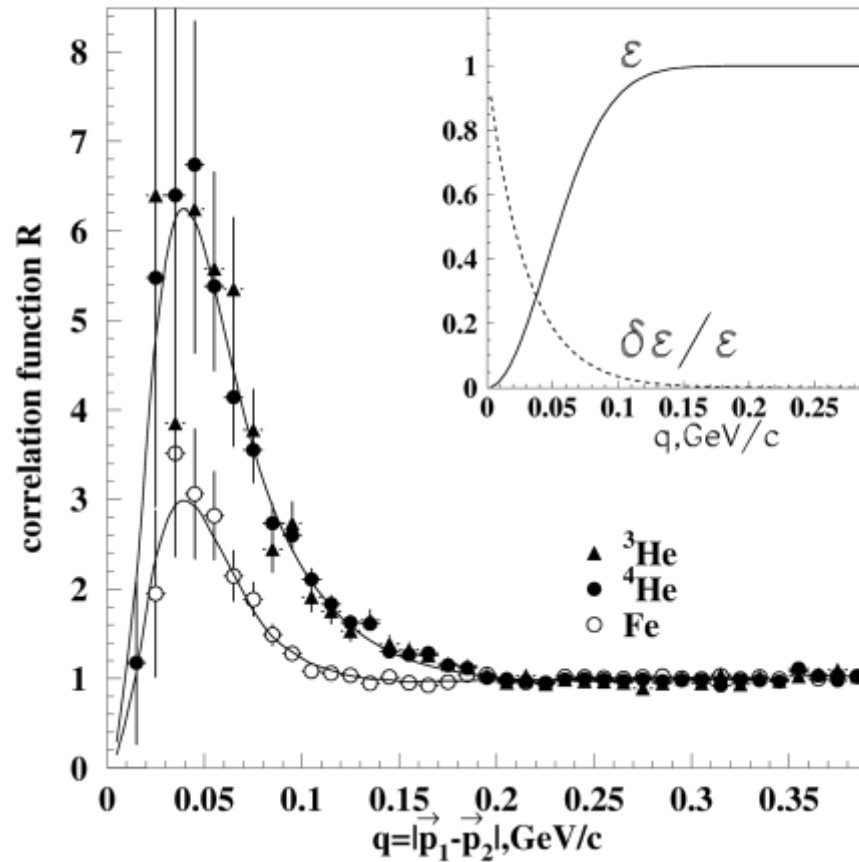
$$R(\vec{p}_1, \vec{p}_2) = \frac{P_2(\vec{p}_1, \vec{p}_2)}{P_1(\vec{p}_1) \cdot P_1(\vec{p}_2)}$$

First application with photons: size of stars (R. Hanbury-Brown, R.Q. Twiss, 1956)

In heavy-ion reactions: pions, kaons, protons (Interferometry+strong FSI+Coulomb)...

$$\Delta r = \frac{\hbar c}{\Delta p} = \frac{197 \text{ MeV}/c}{\Delta p} \text{ fm}$$





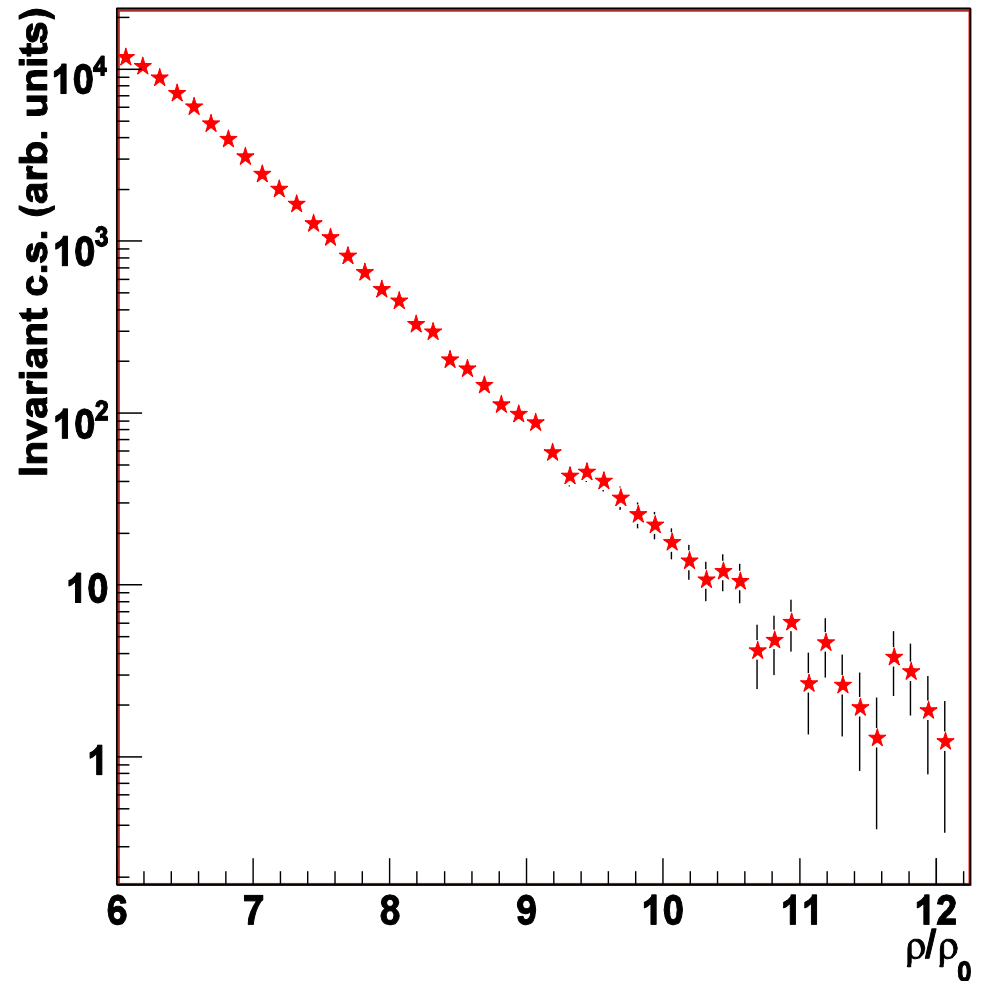
$r_f \sim 1-1.5 \text{ fm}$

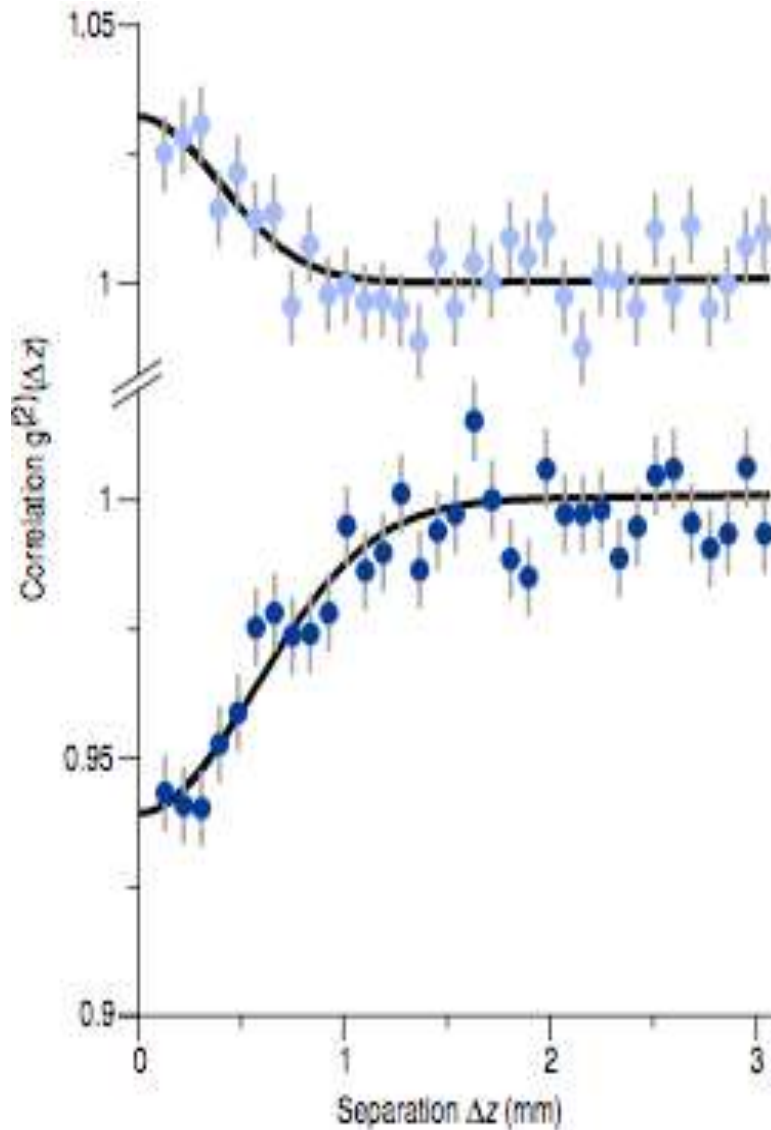
A.S.et al., Phys.Rev.Lett. 93,192301 (2004)



An estimate of baryon density

$r_f \sim 1.5 \text{ fm}$





Caption for figure 2: Normalised correlation functions for 4He^* (bosons) in the upper graph, and 3He^* (fermions) in the lower graph. Both functions are measured at the same cloud temperature ($0.5 \mu\text{K}$), and with identical trap parameters. Error bars correspond to the root of the number of pairs in each bin. The line is a fit to a Gaussian function. The bosons show a bunching effect; the fermions anti-bunching. The correlation length for 3He^* is expected to be 33% larger than that for 4He^* due to the smaller mass. We find $1/e$ values for the correlation lengths of $0.75 \pm 0.07 \text{ mm}$ and $0.56 \pm 0.08 \text{ mm}$ for fermions and bosons respectively.

T.Jeltes et al., Nature, **445**,402(2007)

Hanbury Brown Twiss Effect for Ultracold Quantum Gases

M. Schellekens, R. Hoppeler, A. Perrin, J. Viana Gomes, D. Boiron, A. Aspect, C. I. Westbrook

We have studied two-body correlations of atoms in an expanding cloud above and below the Bose-Einstein condensation threshold. The observed correlation function for a thermal cloud shows a bunching behavior, whereas the correlation is flat for a coherent sample. These quantum correlations are the atomic analog of the Hanbury Brown Twiss effect.

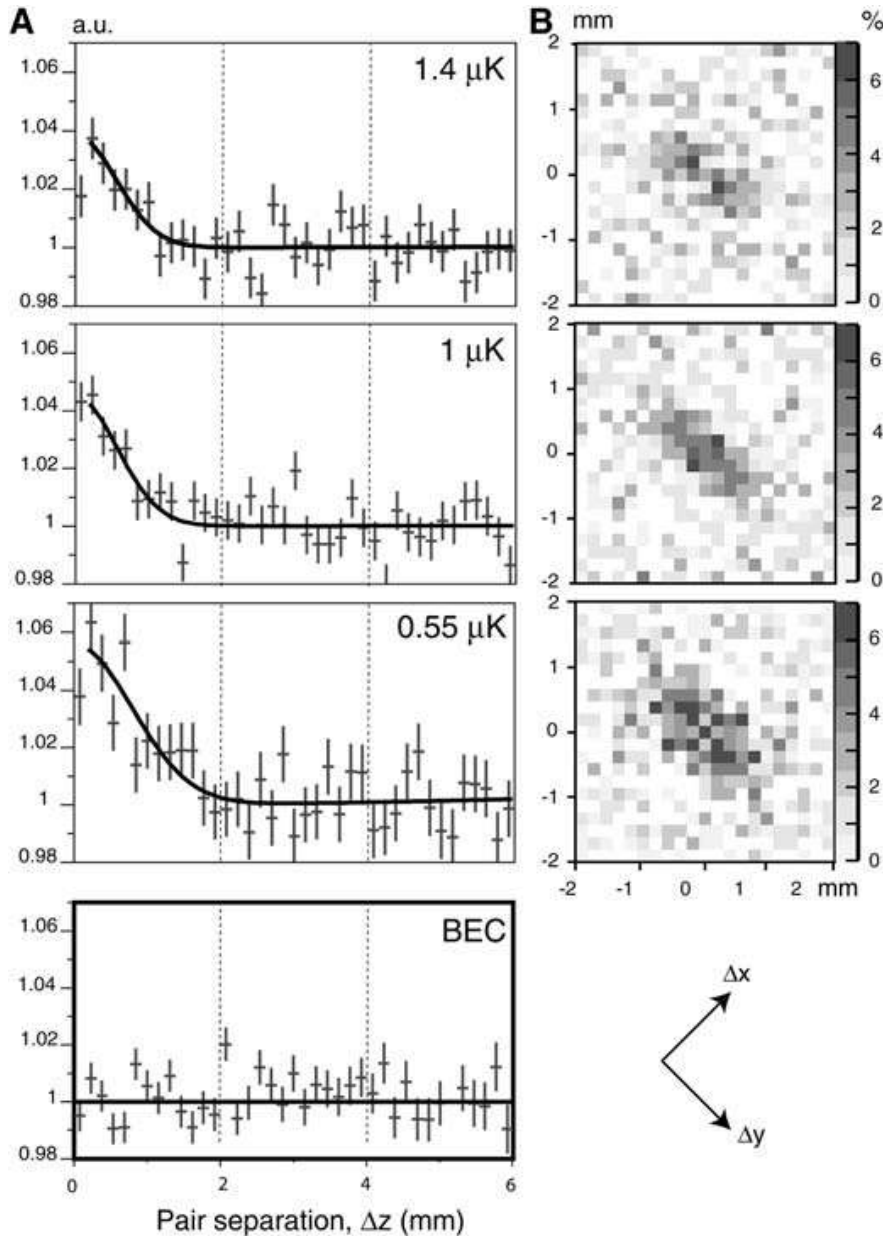
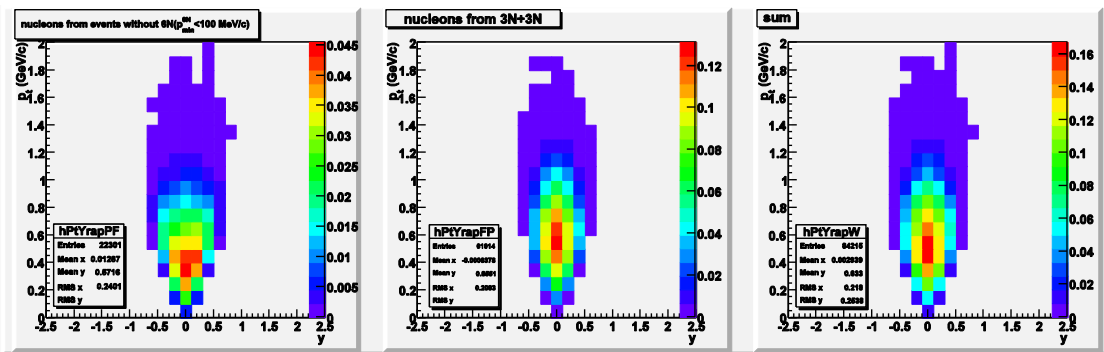


Fig. 2. (A) Normalized correlation functions along the vertical (z) axis for thermal gases at three different temperatures and for a BEC. For the thermal clouds, each plot corresponds to the average of a large number of clouds at the same temperature. Error bars correspond to the square root of the number of pairs. a.u., arbitrary units. (B) Normalized correlation functions in the Δx vs Δy plane for the three thermal gas runs. The arrows at the bottom show the 45-rotation of our coordinate system with respect to the axes of the detector. The inverted ellipticity of the correlation function relative to the trapped cloud is visible.

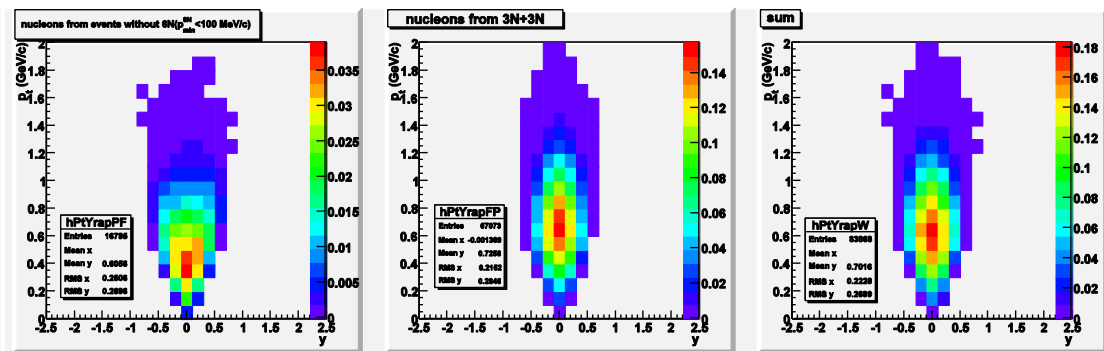
Science, v.310, p.648(2005)

Background and signal, $\sigma_{\text{smear}} = 340 \text{ MeV}/c$

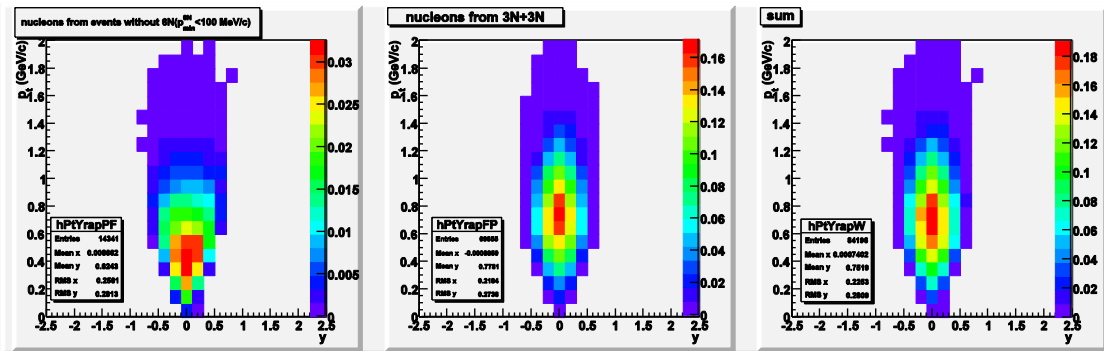
T/A=2.0



T/A=3.2



T/A=4.0



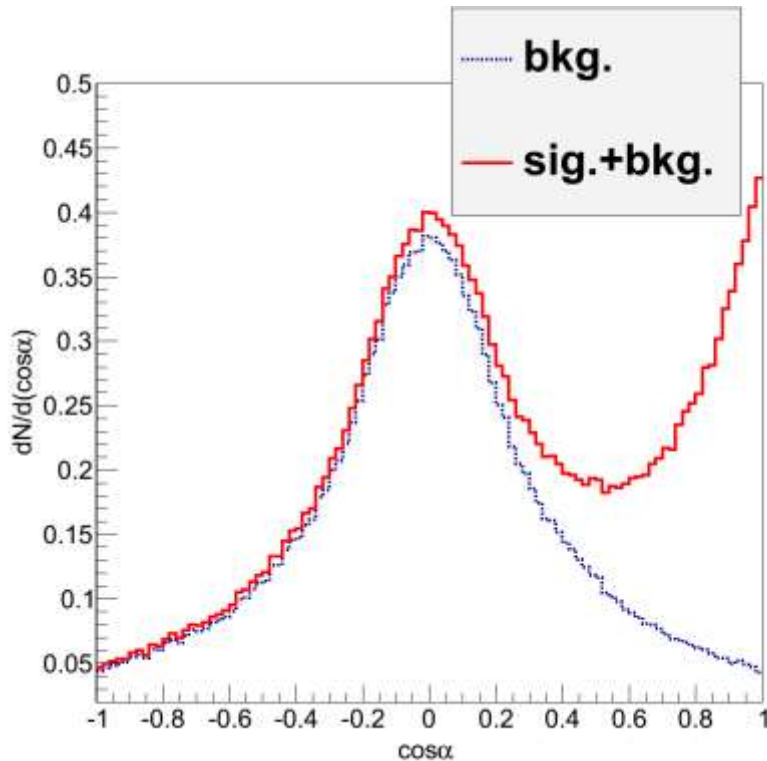
An idea to estimate the background:

- select UrQMD events with the number of nucleon-participants, $N_{\text{prod}} \geq 6$
- among N_{prod} find 6N with minimal momentum, p_{min}
- select events with $p_{\text{min}}^{6N} < p_{\text{cut}}$ (=100 MeV/c)
- remove this 6N from each event, rest nucleons - background
- add the π^0+6N system, these 6N – signal
- momentum of a nucleon from the signal is smearing with a parameter $\sigma_{\text{smear}} = 340 \text{ MeV}/c$ ($\sigma_x = \sigma_y = \sigma_z = \sigma_{\text{smear}}$).

Results: in the region of maximum

T/A (GeV)	S/B
2.0	$\sim 0.12/0.045 = 2.7$
3.2	$\sim 0.14/0.035 = 4$
4.0	$\sim 0.18/0.03 = 6$

Background and signal, $\sigma_{\text{smear}} = 340 \text{ MeV}/c$ (continued)



α -angle between trigger particle and baryon (cms);

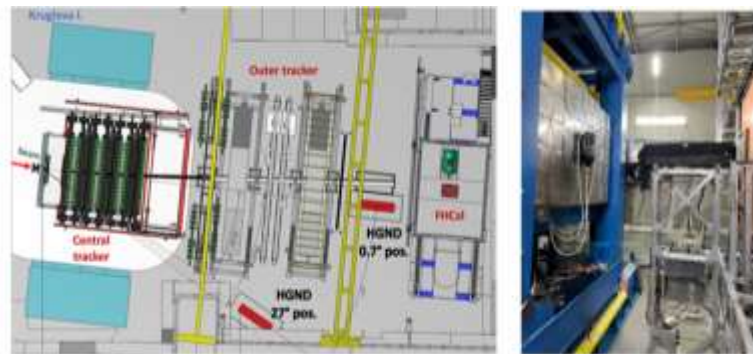
URQMD
CC,
 10^5ev

2 AGeV/c

3 AGeV/c

4 AGeV/c

P	271 961	266 605	266 161
N	271 720	266 368	266 624
π^0	43 878	64 268	85 051
π^+	37 929	55 837	74 365
π^-	37 969	55 702	74 208
K^0	230	1 121	2 398
K^+	235	1 110	2 304
Λ	225	951	1 922
Σ^0	86	468	927
Σ^+	66	372	788
Σ^-	83	362	785
anti K^0	2	45	130
K^-	3	33	130



HGND prototype on BM@N experiment

Highly granulated neutron detector HGND

- allows to measure neutrons in the range $\sim 0.3 - 3 \text{ GeV}$
- Opens possibility to measure Σ^\pm

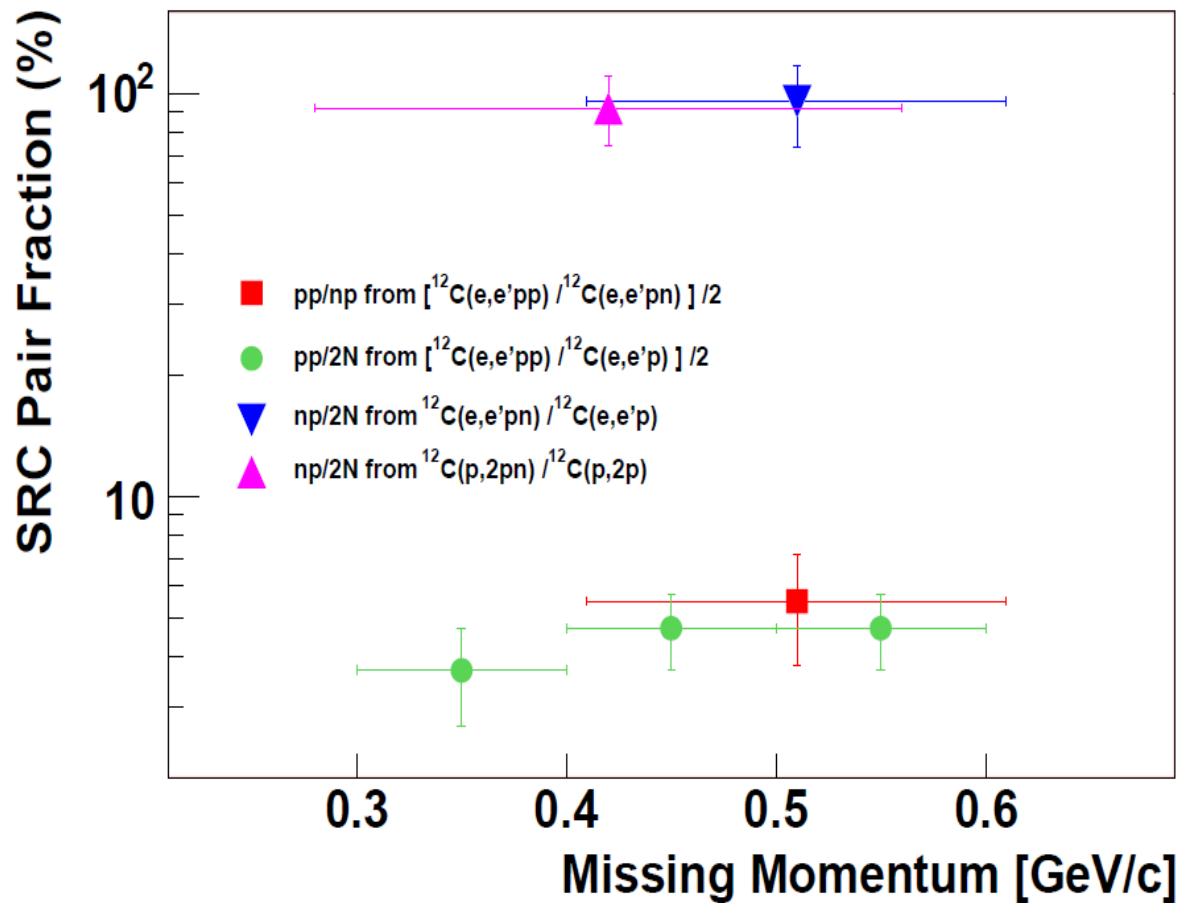
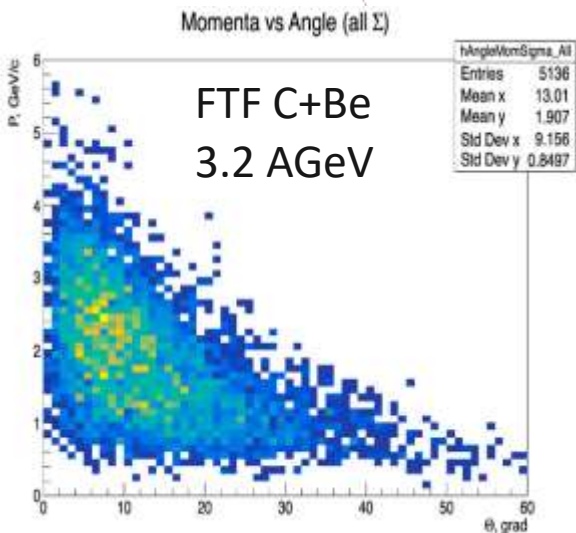
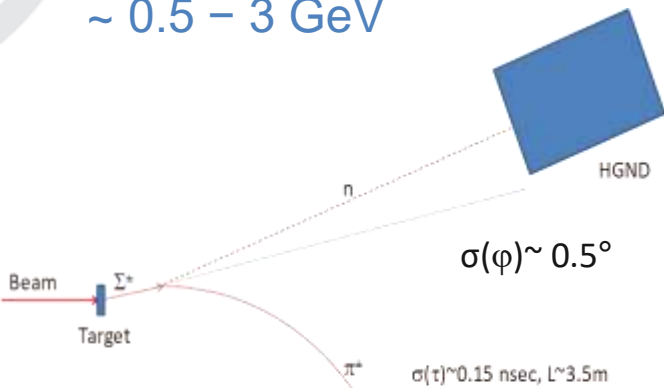


Figure 2: The fractions of correlated pair combinations in carbon as obtained from the (e,e'pp) and (e,e'pn) reactions, as well as from previous (p,2pn) data. The results and references are listed in Table 1.

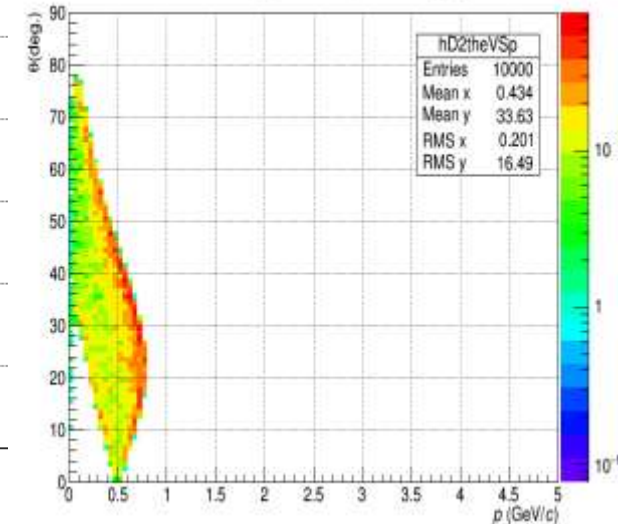
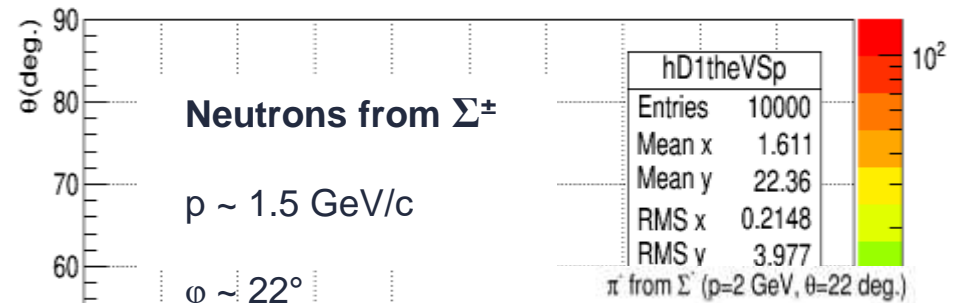
R. Subedi et al., Probing Cold Dense Nuclear Matter,
 arXiv:0908.1514v1 [nucl-ex] 11 Aug
 2009{<http://arxiv.org/abs/0908.1514v1>}.

Neutron detector is important not only for neutron registration, but also for hyperons

E_{kin} of neutrons @ midrapidities is
 $\sim 0.5 - 3 \text{ GeV}$



n from Σ^+ ($p=2 \text{ GeV}, \theta=22 \text{ deg.}$)



Ratio Σ^+/Σ^-

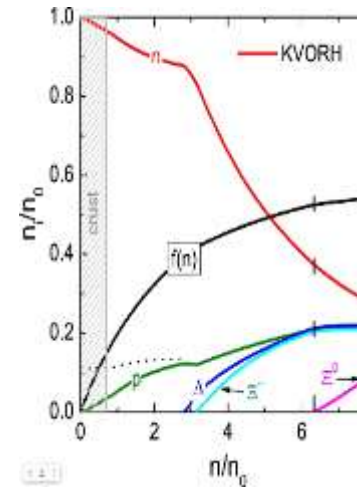
Systematics in Σ^+/Σ^- can be minimized by reversing the magnet

Strangeness in dense nuclear matter and neutron stars

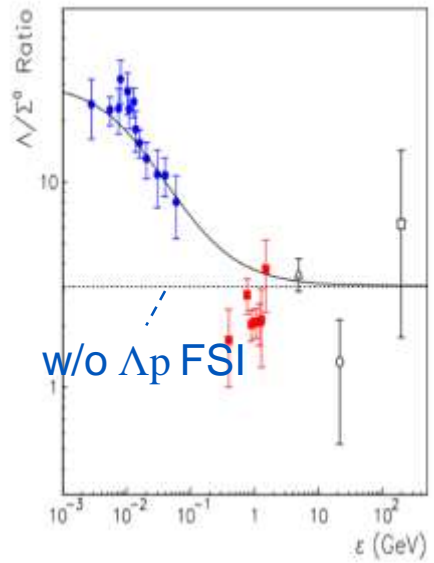
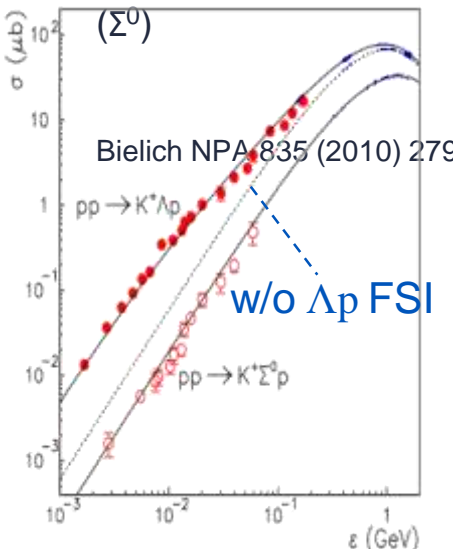
With the increase of density in nuclear stars, the role of Pauli blocking increases

Way out 1* : production of Σ^- (also for compensation of p^+ electrical charge)

Way out 2 : (with further production of Λ : $n \rightarrow \Lambda^0$)



K.A. Maslov , E.E. Kolomeitsev, D.N. Voskresensky PL B748 2015 369



A. Sibirtsev et.al. Eur. Phys. J. A 29, 363–367 (2006)

* ξ

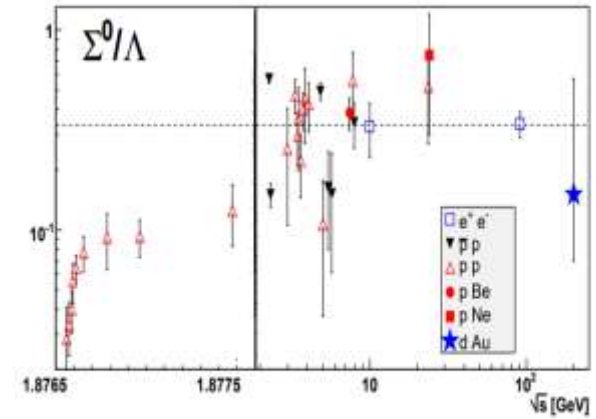
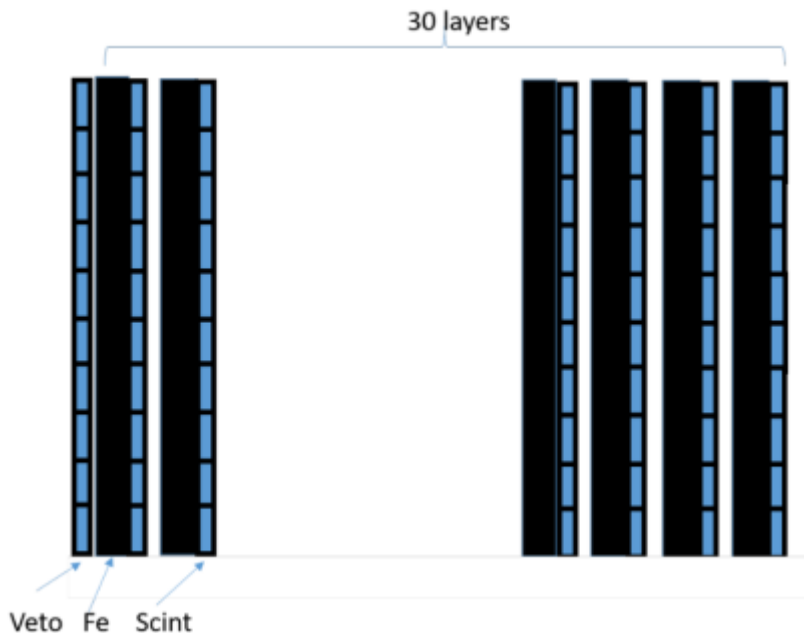


Figure 4: Σ^0/Λ results versus collision \sqrt{s} ($\sqrt{s_{NN}}$ for p/d+A) [1]. Meson-nucleon reaction results are excluded for clarity, but exist only at intermediate energies and lie in the same range. The dashed line is the ratio of isospin degeneracy factors (1/3).

FSI depend on interaction point sizes ($\sim 1/r^2$)
 Λ/Σ ($E \rightarrow 0$) = 30, but Λ/Σ ($E \gg 0$) = 3 for pp.
 Lack of data for AA

G. Van Buren (for the STAR Collaboration) arXiv:nucl-ex/0512018

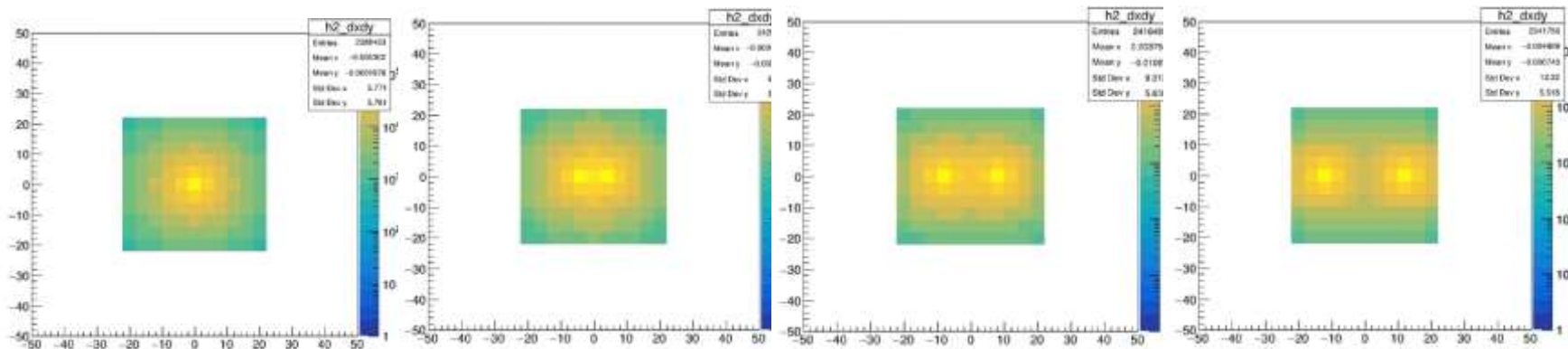
Simulated structure of HighGranularityNeutronDetector:



Structure of Scint. layer:
array of 11x11 scintillator cells 4 x 4 cm²

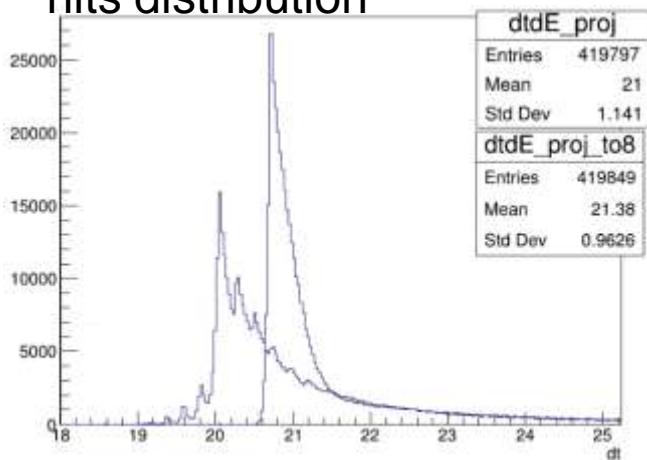
- Transverse size of one layer: 44 x 44 cm²,
- number of layers: – 15 + Veto,
- structure of layer: 3 cm Cu (absorber) + 2.5cm Scint. + 0.5cm (SiPM+FEE)
- size of scintillation detectors (cells): 4x4x2.5 cm³, total number of cells: 1936
- light readout: one SiPM with sensitive area 6 x 6 mm² per cell
- total length of the HGN: ~ 95 cm (~3 λ_{in})

BOX-generator for simulations



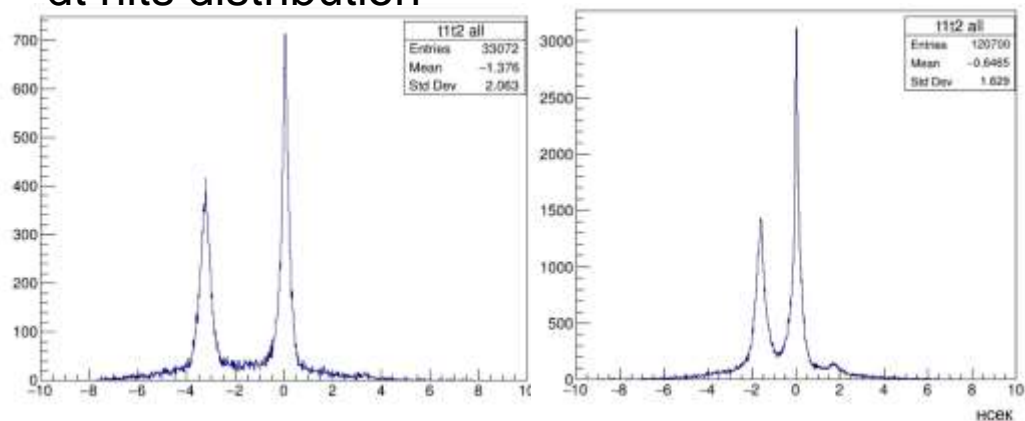
2 Neutron T=1GeV, x-y hits distribution

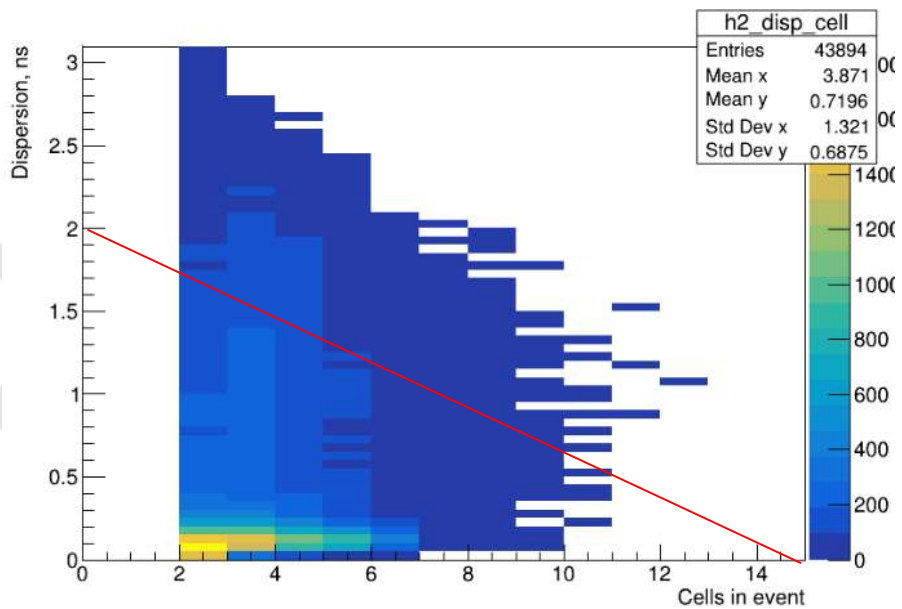
1 Neutron T=1GeV, ToF(L=4m) hits distribution



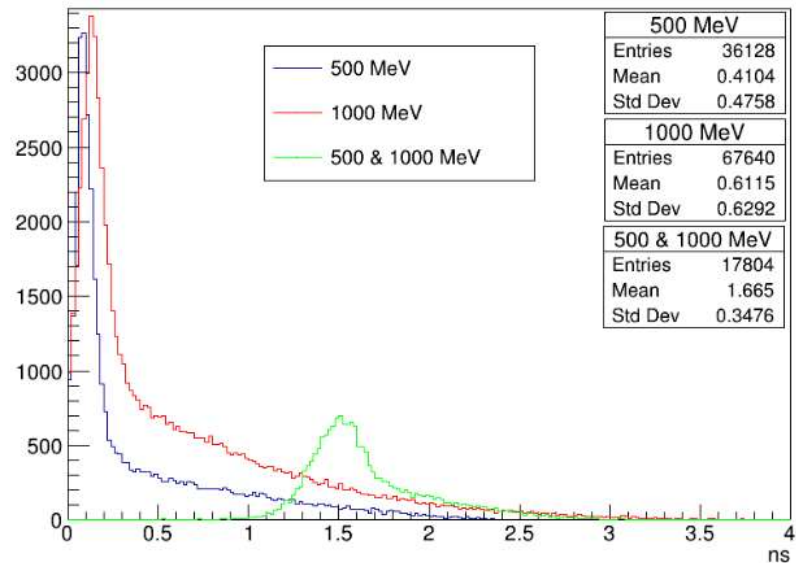
$$t_c = t * d_c / d$$

2 Neutron: T=1GeV and T=0.5GeV(left), T=1Gev and T=2GeV(right); ToF(L=4m) dt hits distribution

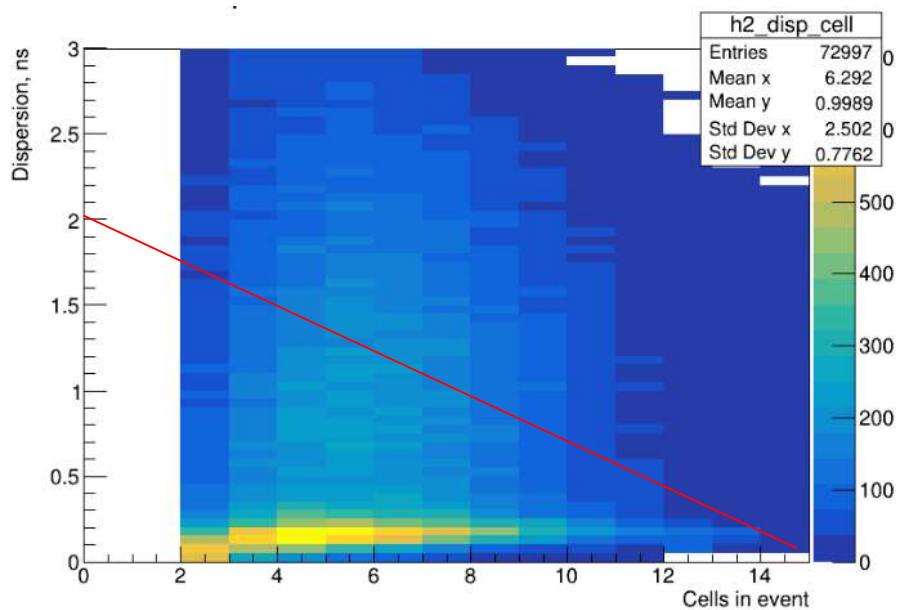




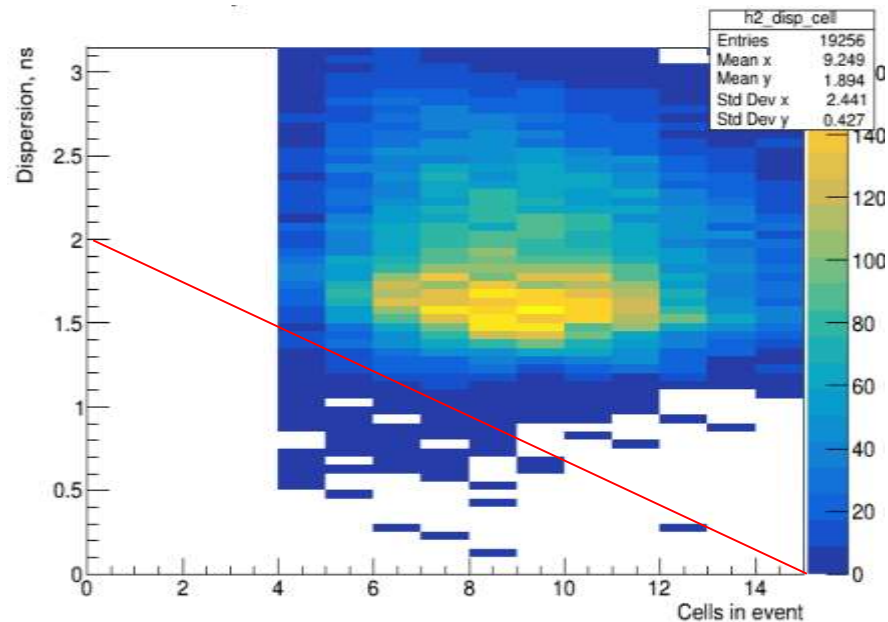
1N, T=0.5GeV



$$D = \sqrt{\frac{\sum(t_i - t)^2}{(n-1)}}$$



1N, T=1GeV



2N, T=0.5GeV and 1GeV

Experimental setup (vesion 0.0)

Targets

p, d, He³,... (incl. polarized)
JINR

Vertex detector

JINR

TOF and Tracker

TOF: $\Delta t < 100\text{ps}$
Tracker: straw(?)

SC toroidal magnet

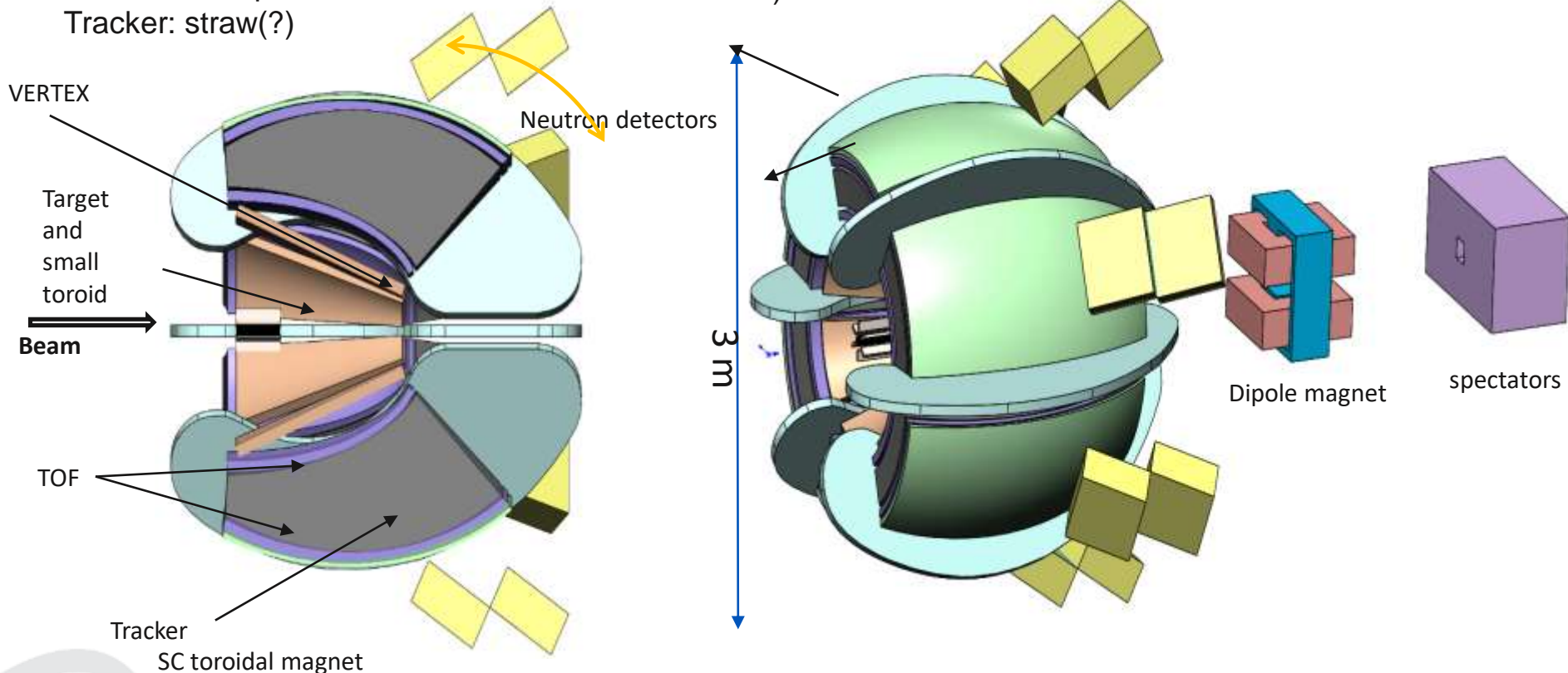
Budker INP RAS

Neutron Detector

- Acceptance ~ 0.25 sr ($\sim 40\%$ full acceptance @ central rapidities)
- Time resolution $< 150\text{ps}$
- $\Delta p/p < 2\%$ \Rightarrow PID, tracking (together with vertex detector)

Dipole magnet and small angles detectors

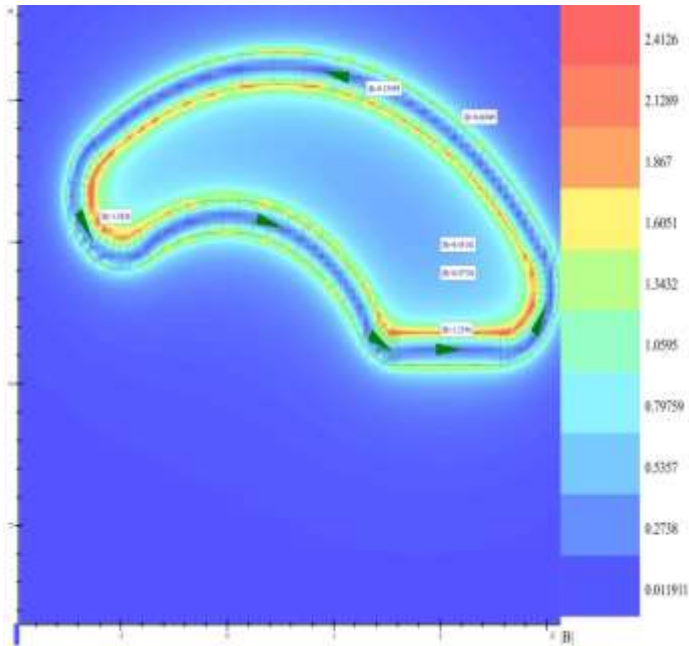
- Spectators registration
- ZDC



SC toroid. Cold vs. High temperature: pros&cons

Cold (He) SC toroid:

- Typical NbTi wires use
- State of art design
- Winding tooling is well established
- Maximum field 2 T is reached
- Larger coil section



magnetic field map

HTSC toroid:

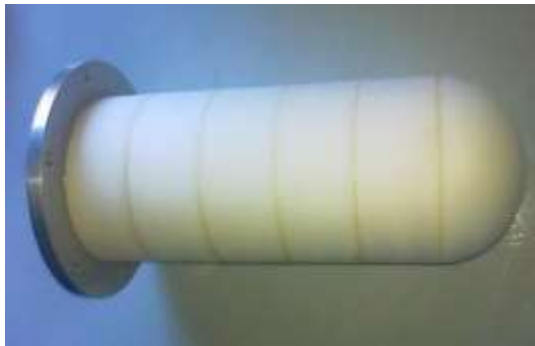
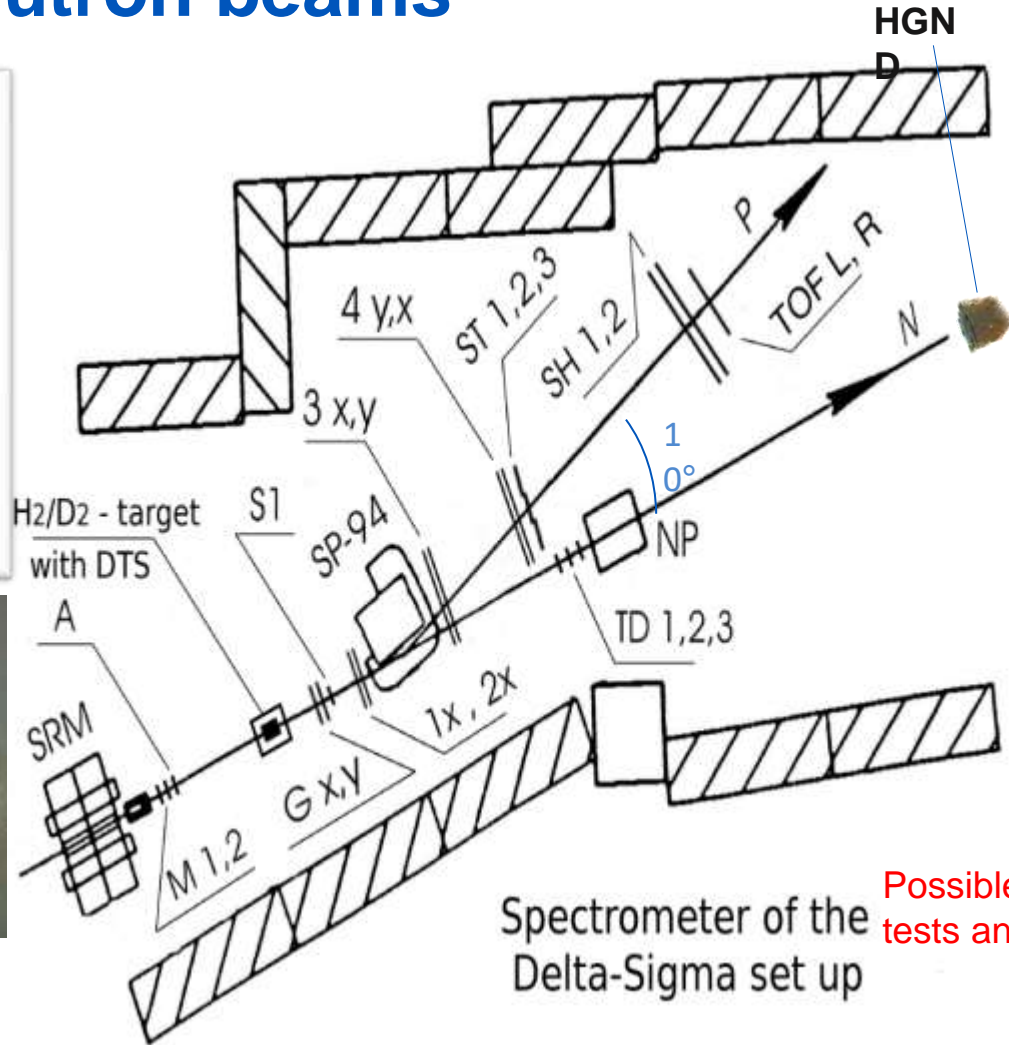
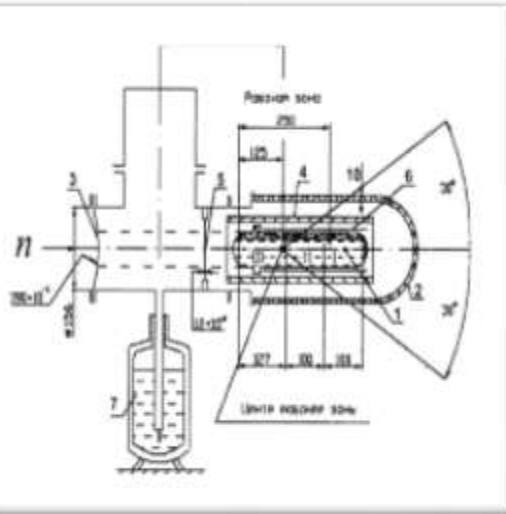
- Need selection for HTSC tapes for uniform and maximum parameters.
- Need work for cable assembling from original tapes
- Winding tooling is not well established
- A lot of design work is required
- Maximum field 2 T is reached only for 40 K temperature use (but cooling equipment for 40 K is commercially available in China for example)
- Maximum field 1.3-1.5 T may be reached for 77 K
- Coil section is smaller for about 30-40 %
- Smaller operation cost



HTSC cable

⇒ Needs development work for both toroid versions to compare and choose the appropriate one.

Delta-Sigma experimental place @ Nuclotron neutron beams



H₂/D₂ Cryogenic target

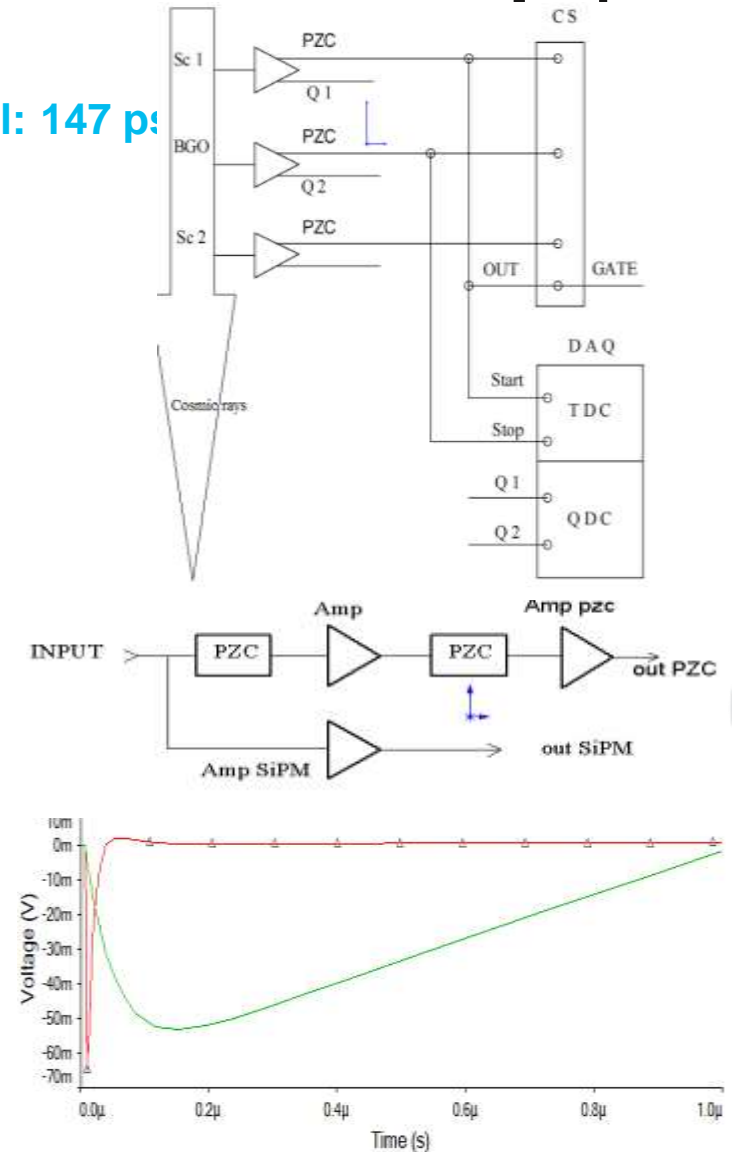
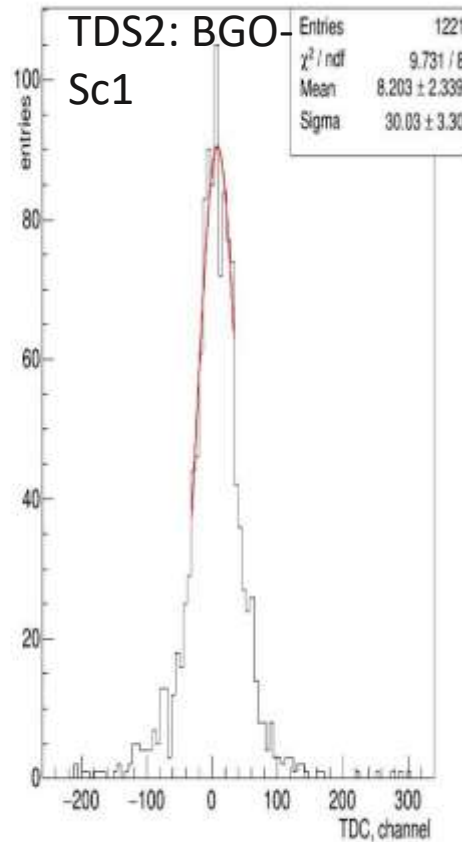
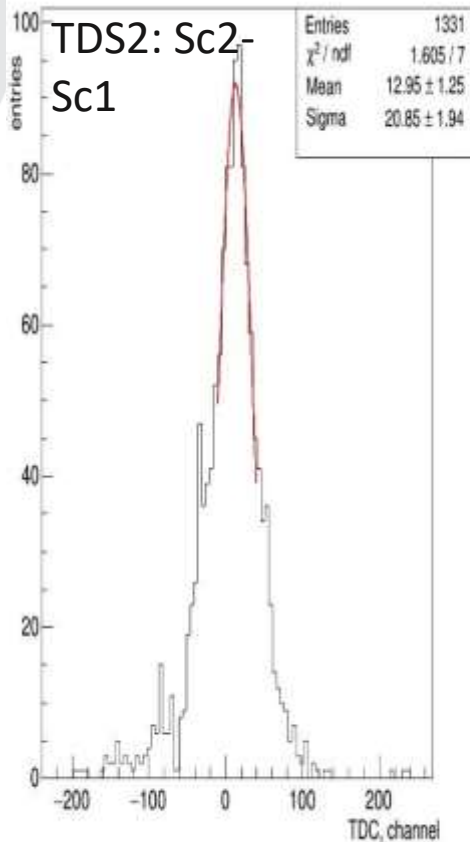
Possible place for HGND tests and calibration

Spectrometer of the Delta-Sigma set up

HGND with active absorber (BGO) Cosmic rays test

Hip_{Ta}N

Time resolution for BGO crystal: 147 ps



35psec

Zero Pole Cancellation scheme

Straw tubes based tracking detector

SPD straw tracker

The straw tracker are using of in the different experiments

“Straw Tracker of the future Spin Physics Detector at NICA collider”
V. Bautin, T. Enik et. al. PoS TIPP2023 (2025) 125)

- Main tracker system of SPD ~2m long, D~1.6 m
- Straw diameter 10 mm, thickness 36 um PET
- Spatial resolution of 150 um
- Barrel is made of 6 modules with up to 30 double-layers, with the ZUV orientation (0,+/-2°)
- Endcaps are made of 12 double-layers with the XYUV orientation
- Rate O(100 kHz)
- ~20000 straws



Straw winding

- ATLAS
- LHCb
- PANDA
- CBM
- COMPASS
- Mu2e
- NA64
- SVD-2
- GLUEX
- COZY-TOF
- ..

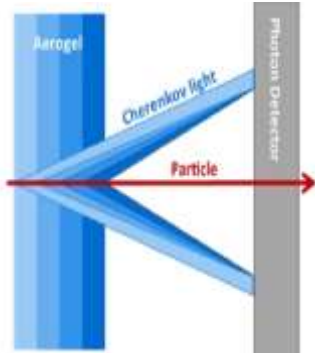
Straw welding

- NA62
- SPD
- KEDR
- COMET
- SHiP
- DUNE
- OKA
- VES
- SPASCH
- ARM
- ..

Aerogel based Cherenkov detectors for future HEP experiments

A. Barnyakov et. al.

Hip_{Ta}N

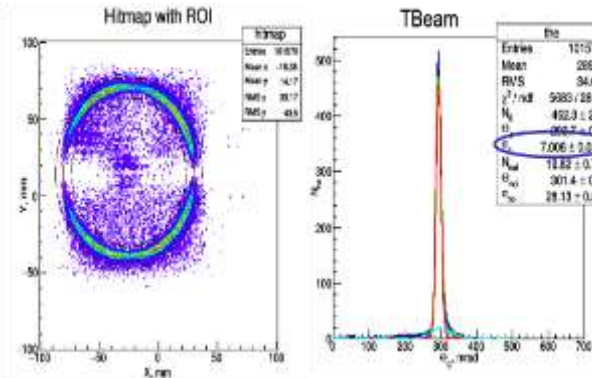
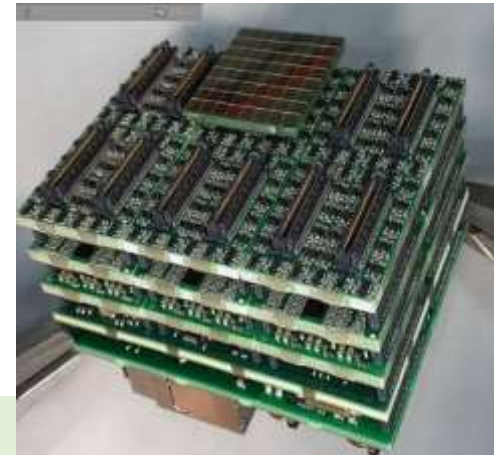


FARICH for reliable π/K and μ/π separation

The technique has been developed since 2004

The most crucial issue now is position-sensitive photon detectors and FEE+DAQ issues.

- π/K –separation up to 8.5 GeV/c
- μ/π –separation up to 1.7 GeV/c
- K/p –separation from 3 to 14 GeV/c



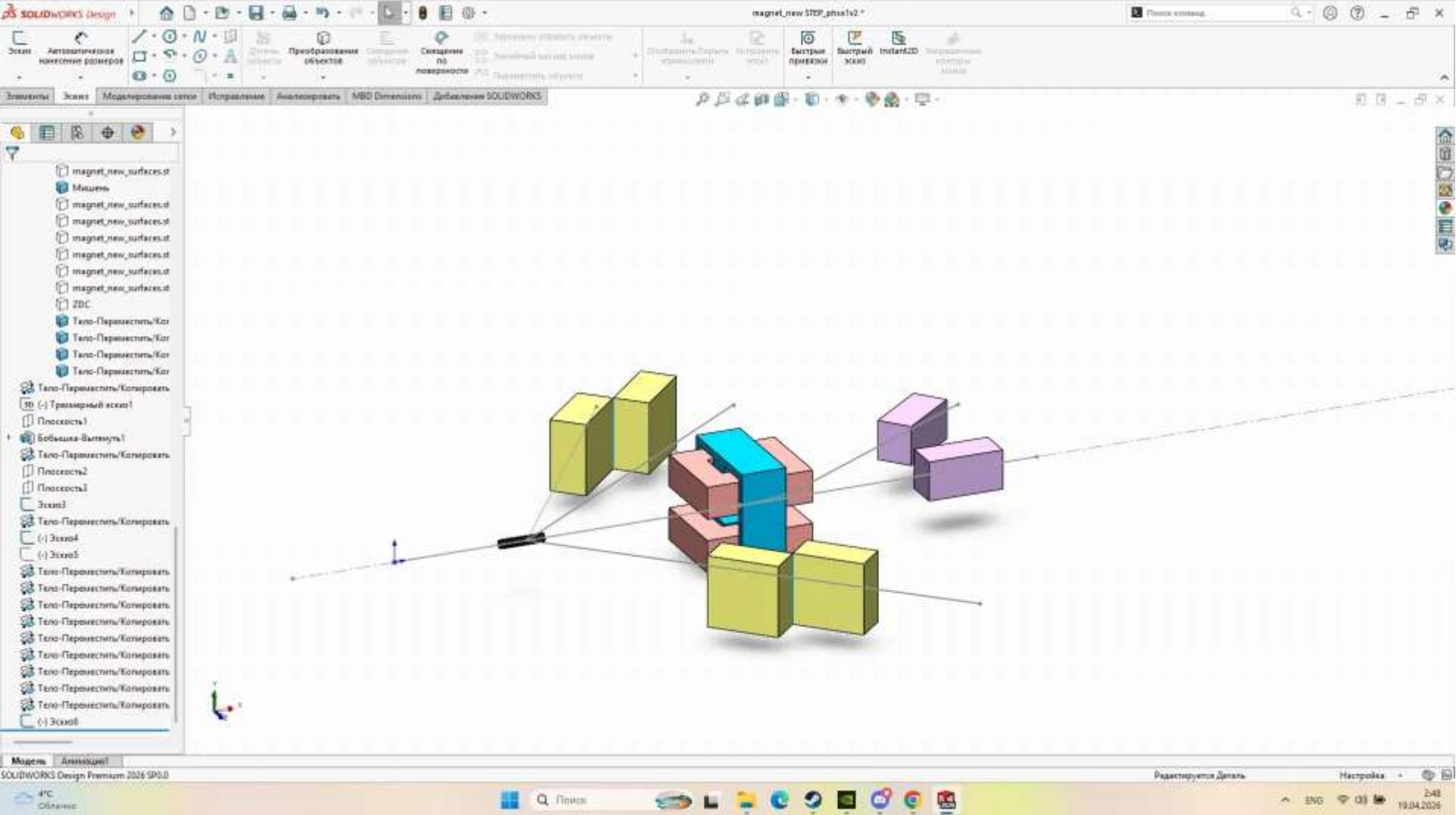
Very promising progress in focusing aerogels production was achieved in 2022-2023. Several the largest 4-layer tiles of the focusing aerogel were produced in Novosibirsk

The beam test results are in good agreement with simulation. The expected (required) angle resolution for single Cherenkov photon was obtained experimentally.

A.Yu. Barnyakov, et al., Nucl. Instr. and Meth. A 553 (2005) 70–75

A.Yu. Barnyakov, et al., Int. J. of Mod. Phys. A 39, No. 26n27, 2442012 (2024)

A.Yu. Barnyakov, et al., Phys. Part. Nucl. 56, No. 3 (2025) 652–655



Hiptan, stage 1

Conclusions

Hip_TaN

- A new experimental program **Hip_TaN** is presented. Investigation of rare processes in high p_T region on fixed targets at Nuclotron is the main goal of the project.
- Unique properties of Nuclotron complex (high intensity, polarized beams, polarized targets) together with the development of new neutron detector open unique possibilities to study npQCD problems and cold dense baryonic matter
- Experimental setup for investigations at high p_T is proposed
 - Modular and comprehensive
 - 3m SC toroid: cold and high temperature versions discussed
 - High Granularity Neutron Detector
 - Algorithms of signal/noise separation
 - Active BGO absorber
 - Straw tubes tracker
 - Aerogel

Extra slides

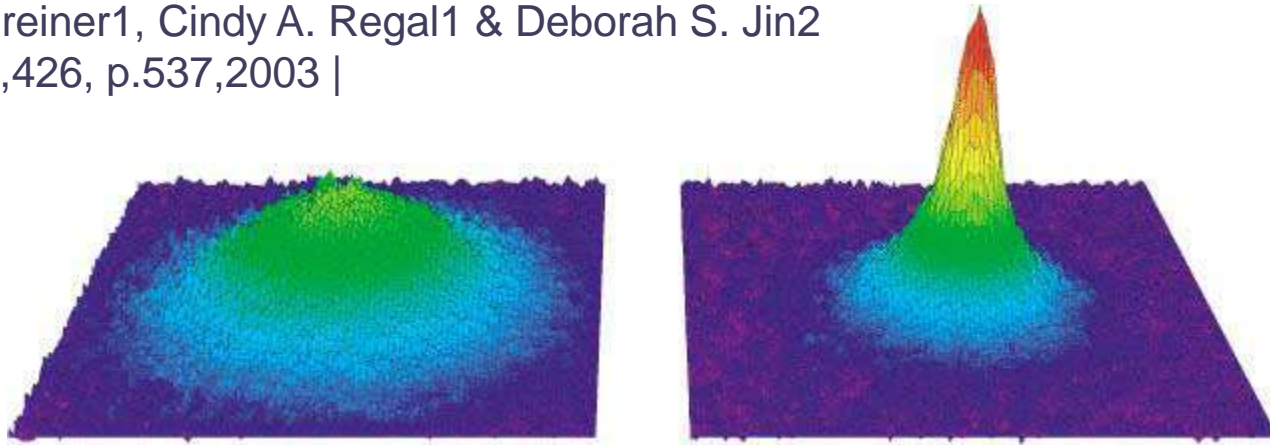


Figure 1 Time-of-flight images of the molecular cloud, taken with a probe beam along the axial direction after 20 ms of free expansion. Data are shown for temperatures above and below the critical temperature for Bose–Einstein condensation. Surface plot of the optical density for a molecule sample created by applying a magnetic-field sweep to an atomic Fermi gas with an initial temperature of $0.19T_F$ ($0.06T_F$) for the left (right) image. The total molecule number was 470,000 (200,000) for the left (right) picture. The surface plots are the averages of ten images.

Rate estimate for DCM trigger (preliminary)



Estimated possible data sample (based on ITEP experimental data):

Nuclotron: $10^6 \text{sec} * 10^8 \text{int/sec} * 0.4 \text{ster}$ $\sim 10^5$ events (CC) for Q1+Q2~6

NICA: $10^6 \text{sec} * 10^5 \text{int/sec} * 10 \text{ster}$ $\sim 1/40$ Nuclotron-rate

CBM@SIS100: $10^6 \text{sec} * 10^8 \text{int/sec} * 1.2 \text{ster}$ ~ 3 Nuclotron-rate

Fermi motion

